Decoding and blocking the bacterial lipid flippase MprF yields a novel anti-virulence strategy

Christoph J. Slavetinsky[1,2,3,4], Janna N. Hauser[1,3,4], Cordula Gekeler[1,3,4], Jessica Slavetinsky[1,3,4], André Geyer[1,3], Alexandra Kraus[5], Doris Heilingbrunner[5], Samuel Wagner[3,4,6], Michael Tesar[5], Christopher Weidenmaier[7], Bernhard Krismer[1,3,4], Sebastian Kuhn[1,3], Christoph M. Ernst[1,3,8] & Andreas Peschel[1,3,4]

[1]Department of Infection Biology, Interfaculty Institute for Microbiology and Infection Medicine Tübingen (IMIT), University of Tübingen, Tübingen, Germany.

[2]Pediatric Gastroenterology and Hepatology, University Children's Hospital Tübingen, Eberhard Karls University Tübingen, Tübingen, Germany.

[3]German Centre for Infection Research (DZIF), Partner Site Tübingen, Tübingen, Germany.

[4]Cluster of Excellence "Controlling Microbes to Fight Infections," University of Tübingen, Tübingen, Germany.

[5]MorphoSys AG, Martinsried, Germany.

[6]Section of Cellular and Molecular Microbiology, Interfaculty Institute for Microbiology and Infection Medicine Tübingen (IMIT), University of Tübingen, Tübingen, Germany.

[7]Interfaculty Institute for Microbiology and Infection Medicine Tübingen (IMIT), University of Tübingen, Tübingen, Germany.

[8]Present address: Christoph M. Ernst, Department of Molecular Biology and Center for Computational and Integrative Biology, Massachusetts General Hospital, Harvard Medical School, Boston, Massachusetts, USA.

Correspondence to **Christoph J. Slavetinsky**, University Children's Hospital, Hoppe-Seyler-Straße 1, 72076 Tübingen, Germany; Phone: +4970712983781; Mail: christoph.slavetinsky@med.uni-tuebingen.de or **Christoph M. Ernst**, Harvard University, Broad Institute, 415 Main Street, Cambridge MA 02142, USA; Mail: cmernst@broadinstitute.org.

Conflict of interest statement

Antibodies disclosed in the manuscript are part of active patent "Anti-staphylococcal antibodies" (US9873733B2 / EP2935324B1) from A.P., C.M.E., A.K., M.T., assigned to the Universitaetsklinikum Tuebingen and MorphoSys AG. The authors have declared that no further conflict of interest exists.

Abstract

The pandemic of antibiotic resistance represents a major human health threat demanding new antimicrobial strategies. MprF is synthase and flippase of the phospholipid lysyl-phosphatidylglycerol that increases virulence and resistance of methicillin-resistant *Staphylococcus aureus* (MRSA) and other pathogens. With the aim to design an anti-virulence strategy for staphylococci causing minimal antibiotic selection pressure, we developed MprF-targeting monoclonal antibodies which bound and inhibited the MprF flippase. Antibody M-C7.1 targeted a loop in the enigmatic flippase domain that proved to be exposed at both sides of the bacterial membrane, thereby providing mechanistic insights into bacterial lipid translocation. M-C7.1 rendered MRSA susceptible to host antimicrobial peptides and antibiotics such as daptomycin. Moreover, it impaired MRSA survival in human phagocytes and virulence in a murine infection model, which recommends MprF inhibitors for new anti-MRSA approaches. MprF-directed monoclonal antibodies provide a proof of concept for development of precisely targeting anti-virulence drugs which block bacterial defense mechanisms.

Introduction

The continuous increase of antibiotic resistance rates undermines the significance and efficacy of available antibiotics against bacterial infections (Ardal, Balasegaram et al., 2020). Several opportunistic antibiotic-resistant bacterial pathogens including methicillin-resistant *Staphylococcus aureus* (MRSA), vancomycin-resistant enterococci, and extended-spectrum beta-lactam or carbapenem-resistant proteobacteria impose a continuously growing pressure on modern healthcare systems (Tacconelli, Carrara et al., 2017). MRSA is responsible for a large percentage of superficial and severe bacterial infections and the available last-resort antibiotics are much less effective than beta-lactams (Lee, de Lencastre et al., 2018). Unfortunately, no new class of antibiotics has entered the clinical phase since the introduction of the lipopeptide antibiotic daptomycin in 2003 (Ardal et al., 2020). Novel anti-infective strategies that would circumvent on one hand the difficulties in

61 identifying new microbiota-preserving small-molecule antimicrobials and, on the other hand, the
62 enormous selection pressures exerted by broad-spectrum antibiotics, are discussed as potential
63 solutions against a looming post-antibiotic era (Dickey, Cheung et al., 2017). Such strategies could be
64 based for instance on therapeutic antibodies or bacteriophages, which usually have only a narrow
65 activity spectrum. A possible direction could be the inhibition of bacterial targets that are of viable
66 importance only during infection (Lakemeyer, Zhao et al., 2018). Blocking such targets by so-called
67 anti-virulence or anti-fitness drugs would preserve microbiome integrity and create selection
68 pressure for resistance-conferring mutations only on invading pathogens. Interfering with bacterial
69 virulence factors should ameliorate the course of infection and enable more effective bacterial
70 clearance by the immune system or by antibiotics.

71 While anti-virulence and anti-fitness therapies are discussed for several of the notoriously antibiotic-
72 resistant bacterial pathogens, none has passed an early experimental stage, probably because most
73 of the major pharmaceutical companies have strongly reduced their investments into new
74 antibacterials (Ardal et al., 2020, Theuretzbacher, Outterson et al., 2019). A recent approach showed
75 promising effects reducing host colonization and invasion in meningococcal disease using
76 phenothiazines, a family of compounds applied for treatment of psychotic disorders, to target Type
77 IV pili, important bacterial adhesion and virulence factors (Denis, Le Bris et al., 2019). Most of the
78 documented anti-virulence approaches appear to rely on small-molecule inhibitors, which are
79 difficult to identify and often have problematic pharmacological, toxicological, and resistance-
80 inducing properties (Theuretzbacher et al., 2019). Monoclonal antibodies (mABs) directed against
81 anti-virulence targets could be interesting alternatives provided the target can be reached by
82 comparatively large antibody molecules. Therapeutic mABs are used in several malignant and
83 inflammatory diseases(Qu, Tang et al., 2018) and have proven efficacy in toxin-mediated bacterial
84 infections such as anthrax or clostridial toxin-mediated diseases (Chen, Moayeri et al., 2011, Dickey
85 et al., 2017, Posteraro, Pea et al., 2018). Apart from toxin neutralization, however, mABs have hardly
86 been applied in antimicrobial development programs.

87 The Multiple Peptide Resistance Factor (MprF), a large integral membrane protein, is crucial for the
88 capacity of bacterial pathogens such as *S. aureus* to resist cationic antimicrobial peptides (CAMPs) of
89 the innate immune system and CAMP-like antibiotics such as daptomycin (Ernst & Peschel, 2011,
90 Peschel, Jack et al., 2001, Slavetinsky, Kuhn et al., 2016). MprF is highly conserved and can be found
91 in various Gram-positive or Gram-negative pathogens (Slavetinsky et al., 2016). MprF proteins
92 proved to be crucial for *in vivo* virulence of various pathogens in infection models and when exposed
93 to human phagocytes(Slavetinsky et al., 2016). Some parts of the protein are located on the outer
94 surface of the cytoplasmic membrane and could in principle be reached by mABs (Ernst, Kuhn et al.,
95 2015, Ernst, Staubitz et al., 2009). MprF forms oligomers and it is a bifunctional enzyme, which can
96 be separated into two distinct domains (Ernst et al., 2015). The C-terminal domain synthesizes
97 positively charged lysyl-phosphatidylglycerol (LysPG) from a negatively charged phosphatidylglycerol
98 (PG) acceptor and a Lys-tRNA donor substrate, while the N-terminal domain translocates newly
99 synthesized LysPG from the inner to the outer leaflet of the cytoplasmic membrane (Ernst et al.,
100 2009, Roy & Ibba, 2009). The exposure of LysPG at the outer surface of the membrane reduces the
101 affinity for CAMPs and other antimicrobials (Ernst et al., 2009). Notably, *mprF* is a major hot spot for
102 point mutations that lead to daptomycin resistance acquired during therapy of *S. aureus* infections
103 (Ernst, Slavetinsky et al., 2018).

104 In order to assess the suitability of MprF as a target for anti-virulence agents we developed mABs
105 targeting several epitopes of potential extracellular loops of its transmembrane part and analyzed
106 their capacity to bind specifically to *S. aureus* MprF. We identified a collection of mABs, which did not
107 only bind to but also inhibited the LysPG flippase domain of MprF. Our results suggest that a specific
108 loop between two of the transmembrane segments (TMS) of MprF is exposed at both sides of the
109 membrane suggesting an unusual, potentially flexible topology of this protein part, which may be
110 involved in LysPG translocation. Accordingly, targeting this loop with a specific mAB inhibited the
111 MprF flippase function, rendered *S. aureus* susceptible to killing by antimicrobial host peptides and
112 daptomycin, and reduced *S. aureus* survival when challenged by human CAMP-producing

113 polymorphonuclear leukocytes (PMNs). Notably, it attenuated *S. aureus* virulence in a mouse
114 infection model.

115

116 **Results**

117 **1. Generation of mABs binding to putative extracellular loops of MprF**

118 The hydrophobic part of *S. aureus* MprF appears to include 14 TMS connected by loops with
119 predicted lengths between two and 56 amino acids (Ernst et al., 2015). Several of the loops are
120 located at the outer surface of the cytoplasmic membrane, accessible to mABs (Figure 1A). Peptides
121 representing four loops with a minimum length of 13 amino acids were synthesized with N- and C-
122 terminal cysteine residues to allow cyclization (Table S1). The peptides corresponded to three loops
123 predicted to be at the outer membrane surface (loops one, nine, and thirteen) and loop seven, the
124 location of which has remained ambiguous due to conflicting computational and experimental
125 findings (Ernst et al., 2015). The N-terminal amino groups of cyclized peptides were linked to biotin
126 to facilitate their recovery and detection. The antigen peptides were incubated with MorphoSys´s
127 Human Combinatorial Antibody Library (HuCAL), a phage display library expressing single-chain
128 human Fab fragments with highly diverse variable regions at the phage surface (Prassler, Thiel et al.,
129 2011). Antigen-binding phages were enriched in three iterative rounds of panning in solution and
130 antigen-phage complexes were captured with streptavidin-coated beads. The bound phages were
131 extensively washed to remove unspecifically binding phages, eluted, and propagated in *Escherichia*
132 *coli* for a subsequent panning round. Washing steps were prolonged and antigen concentrations
133 reduced from round one to round three to increase stringency and discard antibodies with low
134 specificity and affinity. DNA of the eluted, antigen-specific phages was isolated and subcloned in
135 specific *E. coli* expression vectors to yield His-tagged Fab fragments. 368 individual colonies per
136 antigen were picked and Fab fragments were expressed and purified. A representative selection of
137 24 unique Fabs against all four peptides were converted to human IgG by cloning in an IgG1

138 expression vector system and expression in human HKB11 cells and IgGs were purified via protein A
139 chromatography, as recently described (Prassler et al., 2011) (see graphical workflow in Fig. S1).

140 The IgGs were analyzed for binding to the corresponding antigen peptides and also to the three non-
141 cognate peptides to assess their selectivity, by ELISA with streptavidin-coated microtiter plates (Fig.
142 S2). Antibodies directed against the four targeted MprF loops were selected based on affinity and
143 selectivity and analyzed for binding to *S. aureus* SA113 cells expressing or not expressing MprF. Both,
144 the wild-type (WT) and *mprF* deletion mutant strains lacked the gene for protein A (*spa*), which
145 would otherwise unspecifically bind to IgG (Kim, Thammavongsa et al., 2012). Bacteria were
146 adsorbed to microtiter plates, blocked with bovine serum albumin (BSA), and incubated with IgGs,
147 which were then detected with goat anti-human IgG after extensive washing. Antibodies M-C1, M-
148 C7.1, M-C7.3, M-C9.1, M-C13.1, and M-C13.2 bound significantly stronger to MprF-expressing *S.*
149 *aureus* compared to MprF-deficient *S. aureus*, while the humanized isotype control mAB L-1, directed
150 against chicken lysozyme, showed no specific binding (Fig. 1B). These findings are in agreement with
151 the location of the loops one, nine, and thirteen at the outer surface of the cytoplasmic membrane,
152 confirming the overall topology of MprF (Fig. 1A). Of note, loop seven between potential TMS 7 and 8
153 whose location had previously remained controversial was detected by antibodies M-C7.1 and M-
154 C7.3 (Fig. 1B) indicating that loop seven is accessible from the outside. Antibodies M-C1, M-C7.1, M-
155 C9.1, and M-C13.1 showed the strongest binding to MprF according to mean fluorescence intensities.

156

157 **2. The MprF epitope bound by M-C7.1 is located at both outer and inner surface of the**
158 **cytoplasmic membrane**

159 The MprF loop seven between TMS 7 and 8 bound by M-C7.1 seemed to have an ambiguous position
160 within the cytoplasmic membrane because the flanking TMS have a comparatively low content of
161 hydrophobic amino acids. Accordingly, only some topology analysis algorithms predict its location at
162 the outer surface of the cytoplasmic membrane and a previous experimental topology investigation

163 using a set of translational fusions with enzymes that are active only at intracellular or extracellular
164 location has revealed a preferential location at the inner cytoplasmic membrane surface in *E. coli*
165 (Ernst et al., 2015). Since our M-C7.1, and M-C7.3 binding experiments indicated accessibility of loop
166 seven from the outside, we revisited its location in *S. aureus* with two experimental strategies.

167 To confirm that M-C7.1 has access to its cognate MprF antigen epitope at the outer surface of the
168 cytoplasmic membrane in intact bacterial cells, the *S. aureus* SA113 *spa mprF* double deletion
169 mutant expressing MprF (pRB-MprF) was grown in the presence of M-C7.1. Cells were then
170 disrupted, membranes were solubilized by treatment with the mild non-ionic detergent n-dodecyl-ß-
171 D-maltoside (DDM), and proteins were separated in non-denaturing PAGE gels (blue native PAGE). If
172 M-C7.1 bound before cell disruption and remained tightly attached to MprF, it should shift the MprF
173 bands in Western blots of the blue native gels and be detectable after Western blotting of the blue
174 native gels with a human IgG-specific secondary antibody. In order to detect MprF independently of
175 M-C7.1 an MprF variant translationally fused to green-fluorescent protein (pRB-MprF-GFP), which is
176 detectable by a GFP-specific primary antibody (Ernst et al., 2015), was also used and treated in the
177 same way. To detect potential non-shifted MprF proteins in the native MprF variant (pRB-MprF), M-
178 C7.1 was used as additional primary antibody. *S. aureus* SA113 *spa mprF* double deletion mutant
179 bearing the empty vector (pRB) was used as a negative control. In addition to M-C7.1, all three *S.*
180 *aureus* strains were also incubated with the control antibody L-1. *S. aureus* cells expressing either
181 unmodified MprF or MprF-GFP yielded a protein band migrating at a molecular weight of around 900
182 kilodaltons (kDa) when preincubated with M-C7.1 but not with L-1 or in the empty vector control
183 (pRB) (Fig. 2A; Fig. S5). In contrast, the empty vector control (pRB) showed an unspecific band at 300
184 kDa when preincubated with M-C7.1 or at 150 kDa when preincubated with L-1 but no MprF-specific
185 band (Fig. 2A; Fig. S5). The 900 kDa band of MprF-GFP was co-detected by M-C7.1 and anti-GFP
186 confirming the identity of MprF (Fig. 2A; Fig. S5). We could recently show that MprF forms oligomers
187 in the staphylococcal membrane, which were migrating at ca. 300 and 600 kDa (Ernst et al., 2015).
188 Bands migrating at similar heights (ca. 250 and 500 kDa) were detected specifically in the MprF-GFP

189 lanes after preincubation with either M-C7.1 or L-1 and only by anti-GFP primary antibodies but not
190 by M-C7.1 as primary antibody (Fig. 2A; Fig. S5) suggesting to represent the oligomerized but not
191 mAB-complexed MprF proteins which were recently shown (Ernst et al., 2015). Therefore, the 900
192 kDa bands represent a shift caused by complex formation with M-C7.1 which confirms that M-C7.1
193 specifically binds MprF loop seven in live *S. aureus* cells. The fact, that M-C7.1 as primary antibody
194 was not able to detect 250 and 500 kDa bands of non-complexed MprF proteins either after
195 preincubation with M-C7.1 or L-1 suggests that the MprF folding structure as in the living
196 staphylococcal cell membrane is changed upon solubilization preventing antibody detection by
197 Western blot. Even more likely, a conformational change that makes loop seven accessible to M-C7.1
198 could only occur in the actively flipping MprF protein which would prevent Western blot detection
199 after solubilization. Thus, MprF loop seven would become accessible for M-C.7.1 only during the Lys-
200 PG translocation process in live *S. aureus*. Of note, the MprF-mAB complex migrating at around 900
201 kDa further indicates that higher-order MprF multimers were shifted by complex formation with M-
202 C7.1. Preferential binding of M-C7.1 to a putative MprF multimer but not monomer suggests that
203 such multimers may represent the active flipping MprF state *in vivo*.

204 The position of MprF loop seven was further investigated by inserting a cysteine residue into the loop
205 and analyzing the capacity of the membrane-impermeable agent Na*-(3-maleimidylpropionyl)-
206 biocytin (MPB) to label cysteines covalently, using the Substituted Cysteine Accessibility Method
207 (SCAM) (Bogdanov, Zhang et al., 2005). MPB treatment of intact *S. aureus* cells should only lead to
208 labelling of extracellular protein portions while blocking cysteines at the outside with 4-acetamido-4'-
209 maleimidylstilbene-2,2'-disulfonic acid (AMS), followed by cell homogenization and addition of MPB
210 should allow to label only protein parts at the inner surface of the membrane according to a previous
211 established method in *E. coli* (Bogdanov et al., 2005). An MprF variant lacking all native cysteine
212 residues was generated to exclude background signals. Cysteine residues in MprF were exchanged
213 against serine or alanine residues to minimize structural or functional changes. Native *S. aureus* MprF
214 contains six cysteines none of which is conserved in MprF proteins from other bacteria suggesting

215 that they do not have critical functions. The cysteine-deficient mutant protein was found to be
216 indeed functional because it conferred an increased level of basic daptomycin non-susceptibility
217 compared to the *S. aureus mprF* deletion mutant (Fig. S3), which depends on intact MprF synthase
218 and flippase activities (Ernst et al., 2009). Cysteines were then inserted into MprF loop seven (T263)
219 and, as a control, into the first intracellular loop (loop two, A99) and the last extracellular loop (loop
220 thirteen, T480), the localization of which had been consistently confirmed by previous computational
221 and experimental analyses (Ernst et al., 2015) (Fig. 1A & 2C). Amino acids for exchange were chosen
222 according to weak effect prediction for functional changes by https://predictprotein.org. The SCAM
223 approach further confirmed the topology of intracellular loop two and extracellular loop thirteen
224 (Fig. 2B), thereby demonstrating that the technique can lead to reliable results in *S. aureus*. Notably,
225 MprF loop seven was found in both locations, at the inner and outer surface of the membrane. This
226 finding corroborates the ambiguous position of loop seven and suggests that this loop may have
227 some degree of mobility in the membrane, which may reflect the lipid translocation process. The
228 finding also clarifies why M-C7.1 has the capacity to bind MprF loop seven at the outer surface of the
229 cytoplasmic membrane.

230

231 **3. MABs binding to putative extracellular loops of MprF render *S. aureus* susceptible to CAMPs**

232 MprF confers resistance to cationic antimicrobials such as the bacteriocin nisin by reducing the
233 negative net charge of the membrane outer surface (Ernst et al., 2009, Peschel et al., 2001). If the
234 mABs would not only bind to but also inhibit the function of MprF, *S. aureus* should become more
235 susceptible to nisin. The six mABs with confirmed specific binding to MprF and the lysozyme-specific
236 control mAB L-1 were analyzed for their capacity to increase the susceptibility of *S. aureus* SA113 to
237 nisin. Bacteria were grown in the presence of one of the mABs and then incubated with nisin at the
238 IC_{50} followed by quantification of viable bacterial cells. Two of the MprF-specific mABs targeting
239 loops seven or thirteen increased the sensitivity of SA113*Δspa* to nisin while the other mABs and the

240 control mAB L-1 had no significant impact (Fig. 3A). MAB M-C7.1 caused the strongest sensitization
241 and was selected for further analysis using the highly prevalent and virulent community-associated
242 methicillin-resistant *S. aureus* (CA-MRSA) USA300 clone (Otto, 2013).

243 M-C7.1 was found to also increase the susceptibility of USA300 to the human CAMP LL-37, a host
244 defense peptide produced by epithelial and phagocyte cells (Pinheiro da Silva & Machado, 2017), and
245 to daptomycin, a lipopeptide antibiotic in clinical use sharing physicochemical and antibacterial
246 properties with CAMPs (Bayer, Schneider et al., 2013), in addition to nisin (Fig. 3B-D). Of note, M-
247 C7.1 also increased the antimicrobial activity of daptomycin against the daptomycin-resistant clinical
248 MRSA isolate DAP-R 703 (Jones, Yeaman et al., 2008) (Fig. 3E), suggesting that M-C7.1 may
249 potentially be able to overcome daptomycin resistance during therapy. M-C7.1 but not the control
250 mAB L-1 was able to inhibit growth of USA300 in the presence of subinhibitory concentrations of
251 nisin (Fig. 3F). Thus, mABs specific for certain extracellular loops of MprF may not only bind to MprF
252 but also inhibit its function.

253

254 **4. M-C7.1 inhibits the flippase function of MprF**

255 M-C7.1 binds MprF at the junction between the LysPG synthase and flippase domains (Fig. 1). The
256 lipid patterns of SA113 treated with M-C7.1 at concentrations that increased the susceptibility to
257 nisin or with the control mAB L-1 were compared but showed no differences indicating that the
258 synthase function of MprF was not inhibited by M-C7.1 (Fig. 4A). The flippase activity of MprF
259 promotes the exposure of positively charged LysPG at the outer surface of the cytoplasmic
260 membrane thereby reducing the affinity for the small cationic protein cytochrome C (Peschel, Otto et
261 al., 1999), which binds preferentially to negatively charged PG, or for calcium-bound annexin V
262 (Yount, Kupferwasser et al., 2009). These model proteins have been shown to allow a sensitive
263 assessment of changes in the surface charge of *S. aureus* in several previous studies (Ernst et al.,
264 2018, Ernst et al., 2009, Slavetinsky, Peschel et al., 2012). Treatment of SA113 with M-C7.1 at

265 concentrations that increased the susceptibility to nisin led to a significant increase in the capacity to
266 bind cytochrome C or annexin V compared to treatment with the control mAB L-1 (Fig. 4B, C) thereby
267 indicating that M-C7.1 inhibits the flippase function of MprF. It is tempting to speculate that the
268 protein region of MprF loop seven and adjacent TMSs may accomplish a crucial function in the
269 process of phospholipid translocation, as suggested by the dynamic localization of loop seven on the
270 cytoplasmic and external faces of the membrane.

271

272 **5. M-C7.1-treatment abrogates *S. aureus* survival in phagocytes and attenuates its virulence in a**
273 **skin abscess model**

274 The capacity of PMNs to kill phagocytosed bacteria does not only rely on the oxidative burst but also
275 on the activity of LL-37 and other CAMPs and antimicrobial proteins (Spaan, Surewaard et al., 2013).
276 The increased susceptibility of M-C7.1-treated *S. aureus* to CAMPs should therefore alter its survival
277 ability in PMNs. CA-MRSA strain USA300 was pretreated with mABs, opsonized with normal human
278 serum, and exposed to human PMNs. Treatment with M-C7.1 or the control mAB L-1 did not alter
279 the rate of PMN phagocytosis, but M-C7.1-treated USA300 cells were significantly more rapidly killed
280 by PMNs than those treated with the control antibody (Fig. 5A, B). This finding reflects our previous
281 reports on reduced survival of MprF-deficient *S. aureus* in PMNs (Kristian, Durr et al., 2003, Peschel
282 et al., 2001) and it suggests that *S. aureus* treatment with M-C7.1 might reduce the capacity to
283 persist in infections. To assess this assumption, CA-MRSA strain USA300 treated with M-C7.1 or
284 control mAB L-1 were injected subcutaneously into the flanks of mice and the abscesses were
285 compared after 1.5 days. Notably, the abscesses of M-C7.1-treated infections were smaller, showed
286 less dermonecrosis, and contained significantly less viable bacteria than those of animals with
287 bacteria treated with control antibody (Fig. 5 C, D & Fig. S4). Thus, treatment with M-C7.1 may help
288 to blunt the virulence of *S. aureus* in invasive infections.

289

290 **Discussion**

291 Monoclonal therapeutic antibodies have proven efficacy for neutralization of bacterial toxins such as
292 *Clostridium botulinum* or *Clostridioides difficile* toxins, and mAB-based therapies targeting the *S.*
293 *aureus* alpha toxins and leukotoxins are currently developed (Dickey et al., 2017, Tabor, Yu et al.,
294 2016). Moreover, therapeutic mABs binding to *S. aureus* surface molecules to promote opsonic
295 phagocytosis have been assessed in preclinical and clinical trials (Missiakas & Schneewind, 2016). In
296 contrast, mABs inhibiting crucial cellular mechanisms of bacterial pathogens have hardly been
297 assessed so far (Zheng, Shang et al., 2019). We developed specific mABs, which can block the activity
298 of *S. aureus* MprF, the first described bacterial phospholipid flippase. Our mABs did not mediate
299 increased internalization of *S. aureus* cells, most probably because the bacterial cell wall is too thick
300 to allow binding of the mAB FC part to phagocyte FC receptors. However, the inhibition of MprF by
301 M-C7.1 sensitized *S. aureus* to CAMPs and daptomycin and promoted killing by human PMNs, which
302 use CAMPs as an important component of their antimicrobial arsenal. Of note, M-C7.1 could
303 decrease bacterial load in murine skin abscesses and prevent the abscesses from progressing into
304 dermonecrosis, which could potentially lead to systemic spread. Specific inhibition of MprF could
305 therefore promote the capacity of human host defense to clear or prevent a *S. aureus* infection and
306 would, at the same time, increase the susceptibility of *S. aureus* to CAMP-like antibiotics such as
307 daptomycin. Thus, targeting bacterial defense mechanisms provides a promising concept for anti-
308 virulence therapy.

309 Specific binding of MprF antibody M-C7.1 to the extracellular loop seven inhibited the flippase
310 function of MprF, which indicates that this loop plays a crucial role in the lipid translocation process.
311 Loop seven is located between predicted TMS 7 and 8, and its presence at the outer surface of the
312 cytoplasmic membrane had remained elusive since computational and experimental analyses had
313 yielded conflicting results (Ernst et al., 2015). Surprisingly, we found loop seven to be accessible from
314 both, the outside and inside of the cytoplasmic membrane. This suggests that the protein part
315 formed by loop seven and adjacent TMS 7 and 8 may change its position in the protein complex,

316 moving between the two membrane surfaces to accomplish LysPG translocation (Fig. 6), or it could
317 be in a unique position of the large MprF protein complex that allows access from both sides. This
318 protein part might represent the center of the MprF flippase establishing the previously reported
319 MprF-dependent distribution of charged LysPG in the inner and outer leaflet of the cytoplasmic
320 membrane of *S. aureus* (Ernst et al., 2009) (Fig. 6). Interestingly, in living staphylococcal cells, M-C7.1
321 bound to putative higher-order MprF multimers as shown via blue native Western blotting
322 suggesting that such multimers might represent the active lipid translocating state of MprF.
323 Replacement of conserved amino acids in the M-C7.1-targeted protein part has been shown to
324 inhibit the flippase function of MprF (Ernst et al., 2015), which underscores the crucial function of
325 this domain. Notably, one of the conserved and essential amino acids in TMS 7, D254, is negatively
326 charged. It is tempting to speculate that D254 may interact with the positively charged head group of
327 LysPG during the translocation process. Mutations on loop seven and adjacent TMS have recently
328 been found to cause specific resistance to the structurally related lipopeptide antibiotics daptomycin
329 and friulimicin B but not to other antimicrobials (Ernst et al., 2018). Indirect evidence has suggested
330 that these mutations allow the flippase to translocate these lipopeptide antibiotics instead of or
331 together with LysPG (Ernst et al., 2018), which is in agreement with a direct role of loop seven in the
332 translocation process. A mAB binding loop thirteen also sensitized *S. aureus* to nisin in a similar but
333 less pronounced way as M-C7.1 suggesting that this loop may also have a critical role for MprF
334 activity.

335 With the severe shortage of new antibiotic target and drug candidates, crucial cellular machineries
336 conferring fitness benefits during infection rather than accomplishing essential cellular functions
337 should be considered as targets for the development of new therapeutics. The phospholipid synthase
338 and flippase MprF may become a role model for further targets for such anti-fitness or anti-virulence
339 drugs. Compared to other potential targets, MprF has the advantage that essential parts of it are
340 exposed at the external surface of the cytoplasmic membrane. Moreover, MprF is found in many
341 other bacterial pathogens for which similar therapeutic mABs could be developed (Ernst et al., 2009).

342 On the other hand, only a few amino acids in loop seven are conserved in other bacteria, which
343 would limit the impact of loop-seven-directed mABs on other microbiome members thereby
344 minimizing the resistance selection pressure and the risk of dysbiosis.

345

346 **Materials and Methods**

347 ***Bacterial strains, maintenance and mutagenesis of mprF***

348 We used commonly used strains, the methicillin-susceptible laboratory strain *S. aureus* SA113 (ATCC
349 35556), methicillin-resistant clinical clone *S. aureus* USA300, and the SA113 *mprF* knock-out
350 derivative SA113*ΔmprF*, which has been described recently (Peschel et al., 1999, Wang, Braughton et
351 al., 2007) (Tab. S2).

352 For the construction of a protein A mutant (Δ*spa*) the E. coli/S. aureus shuttle vector pKOR1 (Bae &
353 Schneewind, 2006) was used, which allows allelic replacement with inducible counter-selection in
354 staphylococci. Flanking regions of *spa* were amplified from chromosomal DNA of *S. aureus* COL with
355 primer pairs Spa-del_attB1 (ggggacaagtttgtacaaaaaagcaggc**caatattccatggtccagaact; bold: spa**
356 **sequence)** and Spa-del for BglII (gtcg*agatct*ataaaaacaaacaatacacaacg, restriction site italic) as well as
357 Spa-del_attB2 (ggggaccactttgtacaagaaagctggg**atcagcaagaaaacacacttcc; bold: spa flanking sequence)**
358 and Spa-del rev BglII (aaa*agatct*aacgaattatgtattgcaata, restriction site italic). Both PCR products were
359 digested with BglII and subsequently ligated. Without further purification, the ligation product was
360 mixed with equimolar amounts of pKOR1 and *in vitro* recombination was performed with BP clonase
361 Mix (Invitrogen) according to the manufacturer's instructions. The recombination mixture was
362 transferred to chemically competent *E. coli* DH5α and isolated plasmids from the resulting
363 transformants were analyzed by restriction digest. The correct plasmid was isolated from *E. coli*
364 DH5α and used to electroporate competent *S. aureus* RN4220 from which it was again isolated and
365 transferred into *S. aureus* SA113 by electroporation. Allelic replacement was essentially conducted as

366 previously described (Bae & Schneewind, 2006) and resulting deletion mutants were confirmed by
367 PCR.

368 The *S. aureus* SA113 *spa mprF* double mutant was constructed by transducing the gene deletion
369 cassette of the *S. aureus* SA113 *mprF* deletion mutant to the marker-less *spa*-deficient *S. aureus*
370 SA113 mutant using standard transduction protocols. The resulting *S. aureus* SA113 *spa mprF* double
371 deletion mutant was identified by screening for erythromycin resistance conferred by the gene
372 deletion cassette and confirmed by PCR of the deleted genome section. Bacteria were maintained on
373 tryptic soy agar plates.

374 Cysteine substitutions in *mprF* were accomplished by site-directed mutagenesis in *Escherichia coli*
375 using *E. coli*/*S. aureus* shuttle vector pRB474 bearing *mprF,* using the QuickChange II Site-Directed
376 Mutagenesis Kit (Agilent), as described recently (Ernst et al., 2018). Mutated *mprF* derivatives in
377 pRB474*mprF* were transferred into SA113*ΔmprF* and *mprF* expression was mediated by the plasmid-
378 encoded constitutive *Bacillus subtilis* promoter *vegII*. 10 µg/ml chloramphenicol served for
379 maintenance in all plasmid-based studies. A99, T263, and T480 were chosen for exchange against a
380 cysteine residue because of prediction of a weak effect on protein structure in an analysis of
381 functional changes given a single point mutation according to https://predictprotein.org.

382 Plasmids and primers used in this study are given in Table S3 and S4, respectively. Unless otherwise
383 stated, bacteria were cultivated in Mueller-Hinton Broth (MHB, Sigma-Aldrich) with appropriate
384 antibiotics for all experiments.

385

386 ***Antigen selection and antibody production***

387 MprF-derived peptides of interest (Fig. 1 and Tab. S1) were custom-synthesized by JPT Peptide
388 Technologies GmbH (Berlin). An N-terminal and a C-terminal cysteine were added to enable
389 cyclization. Biotin was coupled to the peptide via a 4,7,10-trioxa-1,13-tridecanediamine succinic acid

390 (Ttds)-linker (Ieronymaki, Nuti et al., 2017). Cyclization and coupling of linker and biotin were
391 performed by JPT Peptide Technologies.

392 Recombinant antibodies were generated from the HuCAL PLATINUM® library, as described recently,
393 by three iterative rounds of panning on the antigen peptides in solution and antigen-antibody-phage
394 complexes were captured with streptavidin-coated beads (Dynal M-280) (Prassler et al., 2011, Tiller,
395 Schuster et al., 2013). Fab-encoding inserts of the selected HuCAL PLATINUM phagemids were cloned
396 and expressed in *E. coli* TG1 F-cells, purified chromatographically by IMAC (Bio-Rad) and subcloned in
397 an IgG1 expression vector system to obtain full-length IgG1s by expression in eukaryotic HKB11 cells,
398 as described recently (Prassler et al., 2011). IgGs were purified by protein A affinity chromatography
399 (MabSelect SURE, GE Healthcare) (Prassler et al., 2011).

400 The humanized antibody against chicken lysozyme MOR03207 (Neuber, Frese et al., 2014) served as
401 IgG negative control and was called L-1 in this manuscript.

402

403 ***Peptide and whole-cell ELISAs of MprF specific mABs***

404 Overnight *S. aureus* SA113*Δspa* or SA113*ΔspaΔmprF* cultures grown in MHB were adjusted to OD_{600}
405 0.1 in fresh MHB and grown to OD_{600} of at least 1.0. Cells were harvested, adjusted to OD_{600} 0.5 with
406 0.9% NaCl, and used to coat 96 well NUNC Maxisorp Immuno Plates for 1 hour (50 µl/well). After
407 three washing steps with Tris-buffered saline (TBS; 50 mM Tris, 150 mM NaCl in 800 mL of H_2O, pH
408 7.4) containing 0.05% Tween 20 (TBS-T), the cells were blocked with PBS containing 1 x ROTI®Block
409 (Carl Roth) for 1 h. Primary antibodies were added after three washing steps with TBS-T at an
410 indicated final concentration of 1, 10 or 100 nM and incubated for 1 h. After three more washing
411 steps with TBS-T, anti-human IgG conjugated to alkaline phosphatase (Sigma-Aldrich A8542) diluted
412 1:10,000 in TBS-T was applied. Finally, after three washing steps with 2x TBS-T and 1x TBS, the cells
413 were incubated with 100 µl p-nitrophenyl phosphate solution as advised by the manufacturer

414 (Sigma-Aldrich N1891). Fluorescence was measured at an excitation of 440±25 nm and an emission
415 of 550±35 nm.

416

417 ***Detection of antibody binding to MprF by blue native Western blotting***

418 To detect binding of the anti-MprF antibody to MprF we performed blue native polyacrylamide gel
419 electrophoresis (BN-PAGE) as previously described (Ernst et al., 2015) with slight modifications.
420 Briefly, 20 ml of *S. aureus* cells grown in MHB with anti-MprF antibodies (100 µg/ml) to OD_{600} 1 were
421 incubated with 750 µl of lysis buffer (100 mM EDTA [pH 8.0], 1 mM $MgCl_2$, 5 µg/ml lysostaphin, 10
422 µg/ml DNase, proteinase inhibitor [cocktail set III from Calbiochem] diluted 1:100 in PBS) for 30 min
423 at 37°C and homogenized three times with 500 µl zirconia-silica beads (0.1 mm diameter from Carl-
424 Roth) using a FastPrep 24 homogenizer (MP Biomedicals) for 30 s at a speed of 6.5 m/s. After
425 removing the beads, cell lysate was centrifuged 20 min at 14,000 rpm and 4°C to sediment cell debris
426 and supernatant was transferred to microcentrifuge polypropylene tubes (Beckman Coulter) and
427 cytoplasmic membranes were precipitated by ultracentrifugation for 45 min at 55,000 rpm and 4°C
428 (Beckman Coulter rotor TLA 55). Membrane fractions resuspended in resuspension buffer (750 mM
429 aminocaproic acid, 50 mM Bis-Tris [pH 7.0]) were incubated with the MprF- or lysozyme-specific
430 humanized IgG mAB and/or a GFP-specific rabbit IgG mAB (Invitrogen) for 30 min shaking at 37°C.
431 Dodecyl maltoside was added to a final concentration of 1% for 1 h at 4°C to solubilize MprF-
432 antibody complexes. Insoluble material was removed by ultracentrifugation for 30 min at 40,000 rpm
433 and 4°C. 20 µl supernatant was mixed 1:10 with 10 × BN loading dye (5% [wt/vol] Serva Blue G, 250
434 mM aminocaproic acid, 50% glycerol) and run on a Novex NativePAGE 4 to 16% Bis-Tris gel
435 (Invitrogen). Separated proteins were transferred to a polyvinyl difluoride membrane and detected
436 via either, goat anti-human IgG DyLight 700 (Pierce) or goat anti-rabbit IgG DyLight 800 (Pierce) as
437 secondary antibodies in an Odyssey imaging system from LI-COR.

438

439 ***Substituted cysteine accessibility method (SCAM) to localize MprF loops in inner and/or outer***
440 ***membrane leaflet***

441 SCAM was adapted for use in *S. aureus* from the protocol recently established for *E. coli* (Bogdanov
442 et al., 2005). Variants of *S. aureus* SA113*ΔmprF* were expressing cysteine-deficient and/or -altered
443 MprF derivatives bearing a FLAG® tag at the C-terminus via the plasmid pRB474. Bacteria were grown
444 at 37°C to an OD_{600} 0.7-0.8 in 100 ml TSB, split into two equal aliquots, and harvested. Pellets were
445 resuspended in a mixture of buffer A (100 mM HEPES, 250 mM sucrose, 25 mM $MgCl_2$, 0.1 mM KCl
446 [pH 7.5]) supplemented with 1 mM $MgSO_4$, 1 mM EDTA, 2.1 µg lysostaphin, 0.7 µg DNase and 1% of a
447 protease inhibitor cocktail (Roche) and incubated for 45 min at 37°C. For staining of cysteine residues
448 in the outer leaflet of the cytoplasmic membrane, cells of the first aliquot were treated with N*-(3-
449 maleimidylpropionyl) biocytin (MPB, Thermo Scientific) at a final concentration of 107 µM for 20 min
450 on ice. In the second aliquot, external cysteine residues were blocked with 107 µM 4-acetamino-4´-
451 maleimidylstilbene-2,2´-disulfonic acid (AMS, Thermo Scientific) for 20 min on ice, bacterial cells
452 were subsequently disrupted in a bead mill as described above and internal cysteines were labeled
453 with MPB for 5 min. MPB labeling was quenched in both aliquots by the addition of 21 mM β-
454 mercaptoethanol. Cell debris was removed by several centrifugation and washing steps, membrane
455 fractions were collected via ultracentrifugation at 38,000 x g, and labeled membrane samples were
456 stored at -80°C.

457 For protein enrichment and precipitation, labeled membrane samples were thawed on ice and
458 suspended in 20 mM β-mercaptoethanol containing buffer A. Proteins were solubilized by the
459 addition of an equal volume of solubilization buffer (50 mM Tris-HCl [pH 9], 1 mM EDTA, 2% SDS) and
460 vigorous vortexing for 30 min at 4°C, followed by an incubation step of 30 min at 37°C and vortexing
461 for 30 min at 4°C. After solubilization, one and a half volumes of immunoprecipitation buffer 1 (50
462 mM Tris-HCl [pH 9], 150 mM NaCl, 1 mM EDTA, 2% Thesit, 0.4 % SDS [pH 8.1]) was added and
463 samples were incubated for 2.5 h with magnetic FLAG®beads (Sigma-Aldrich) in a rotation wheel at
464 4°C. After several washing steps with immunoprecipitation buffer 1 and immunoprecipitation buffer

465 2 (50 mM Tris-HCl [pH 9], 1 M NaCl, 1 mM EDTA, 2% Thesit, 0.4 % SDS [pH 8.1]), FLAG®-tagged MprF
466 was eluted by the addition of 0.1 M glycine-HCl (pH 2.2) and neutralized by adding Tris-HCl (pH 9).

467 For detection of cysteine-labelled MprF, samples were analyzed by denaturing SDS-PAGE and
468 Western blotting. To this end, 12-µl samples were mixed with 4 x Laemmli sample buffer (Bio-Rad),
469 loaded onto a 10%-polyacrylamide gel, and separated via electrophoresis. Proteins were transferred
470 onto a polyvinylidene difluoride (PVDF) membrane (Immobilon-PSQ PVDF membrane, Merck) by
471 semi-dry turbo Western blot procedure (Trans-Blot Turbo Transfer System, Bio-Rad). FLAG®-tagged
472 MprF was detected both by a mouse anti-FLAG® primary antibody (Sigma-Aldrich) and goat anti-
473 mouse secondary antibody (LI-COR) at 700 nm, while MBP-labelled cysteine residues were detected
474 with streptavidin DyLight conjugate (Thermo Scientific) at 800 nm in an Odyssey imaging system from
475 LI-COR.

476

477 ***Determination of susceptibility to antimicrobial agents***

478 Overnight cultures of *S. aureus* SA113*Δspa* or USA300 WT were diluted in fresh MHB and adjusted to
479 OD_{600} 0.25 (~1.5 x 10^7 cells). Antibodies were adjusted to a concentration of 1 mg/ml and 10 µl per
480 well of a 96 well plate were added to 90 µl of the adjusted cell suspension (final antibody
481 concentration: 100 µg/ml). Cells were grown in the presence of the lysozyme-specific control
482 antibody L-1 or with the respective anti-MprF antibodies. After 3 hours of incubation at 37°C under
483 shaking, optical density was determined, and cells were adjusted to OD_{600} 0.025 in 500 µl cold PBS.
484 80 µl of the adjusted cell suspension were mixed with 20 µl of antimicrobial substances to final
485 concentrations of 22.5 µg/ml nisin for SA113*Δspa* or of 5 µg/ml nisin for USA300, 1.5 µg/ml
486 daptomycin for USA300, 11 µg/ml daptomycin for daptomycin resistant CA-MRSA strain 703, and 45
487 µg/ml LL-37 for USA300 or 20 µl PBS as control. After incubation for 2 hours under shaking at 37°C,
488 the cell suspensions were diluted 1:2,000 and 100 µl of each duplicate was plated in triplicates on
489 TSB agar plates to obtain a representative value of bacterial survival.

490 MICs of daptomycin were determined using MIC test strips (Liofilchem) according to the
491 manufacturer's advice.

492 To analyze the capacity of mAB M-C7.1 to inhibit *S. aureus* growth, overnight cultures of CA-MRSA
493 strain USA300 grown in MHB medium were diluted to OD_{600} 0.01 with fresh MHB medium containing
494 1 µM of antibodies and 4 µg/ml nisin (Sigma-Aldrich) or PBS as a control in 96 well plates. Plates were
495 incubated for 24 hours at 37°C under shaking conditions using a Bioscreen C (Oy Growth Curves Ab
496 Ltd). Optical density at 600 nm was determined and compared to growth without nisin.

497

498 ***Isolation and quantification of polar lipids***

499 *S. aureus* cultures (1 ml in MHB) were grown to the exponential phase (OD_{600} 1) in the presence of
500 antibodies (final concentration: 100 µg/ml) as described above for the determination of susceptibility
501 to antimicrobials. Polar lipids were extracted using the Bligh-Dyer method (Bligh & Dyer, 1959), with
502 chloroform/methanol/sodium acetate buffer (20 mM) (1:1:1, by vol.), vacuum-dried, and
503 resuspended in chloroform/methanol (2:1, by vol.). Extracts were filled into a 100-µl Hamilton
504 syringe and spotted onto silica gel 60 F254 high-performance thin-layer chromatography (HPTLC)
505 plates (Merck) with a Linomat 5 sample application unit (Camag) and run in a developing chamber
506 ADC 2 (Camag) with a running solution composed of chloroform-methanol-water (65:25:4, by vol.).
507 Phosphate group-containing lipids were detected by molybdenum blue staining and phospholipids
508 were quantified in relation to total phospholipid content by determining lipid spot intensities
509 densitometrically with ImageJ (http://rsbweb.nih.gov/ij/docs/guide/index.html) as described
510 recently (Slavetinsky et al., 2012).

511

512 ***Determination of S. aureus cell surface charge***

513 For analysis of the cytochrome C repulsion capacity of *S. aureus*, bacterial cells were grown in the
514 presence of antibodies (100 µg/ml) as described above for the analysis of antimicrobial susceptibility.
515 Bacteria were adjusted to OD_{600} 1 in 1 ml PBS, pelleted, resuspended in 100 µl 0.05 mg/ml
516 cytochrome C (Sigma-Aldrich) followed by incubation at 37°C under shaking. The cells were then
517 pelleted by centrifugation and absorption of the supernatant containing unbound cytochrome C was
518 determined at OD_{410}

519 To determine annexin V binding to *S. aureus,* bacterial cells were grown in the presence of antibodies
520 (100 µg/ml) as described above at 37°C with shaking for 3 hours, harvested, washed twice in PBS
521 buffer, and resuspended in PBS containing $CaCl_2$ to OD_{600} 0.5 in 1 ml. Bacteria were gently mixed with
522 5 µl of allophycocyanin (APC)-labeled annexin V (Thermo Scientific) and incubated at room
523 temperature for 15 min in the dark, as described recently (Ernst et al., 2018). At least 50,000
524 bacterial cells per antibody were analyzed by flow cytometry to quantify surface-bound fluorophore
525 (FL-4).

526

527 ***Phagocytosis and killing of S. aureus by human polymorphonuclear leukocytes (PMNs)***

528 Human PMNs are the major human phagocytes to counteract bacterial infection and form the largest
529 subgroup (~95%) of PMNs (Spaan et al., 2013). PMNs were isolated from fresh human blood of
530 healthy volunteers by standard Ficoll/Histopaque gradient centrifugation as described recently
531 (Hanzelmann, Joo et al., 2016). Cells were resuspended in HBSS containing 0.05% human serum
532 albumin (HBSS-HSA; HBSS with 0.05% Albiomin®, Biotest AG).

533 CA-MRSA strain USA300 was prepared for PMN experiments as described for the determination of
534 susceptibility to antimicrobials, grown in the presence of antibodies (100 µg/ml) at 37°C under
535 shaking for 3 hours, harvested, washed twice in HBSS, and adjusted to a density of 5×10^7 CFU/ml.
536 Pooled serum from healthy human volunteers (blood bank of the University Hospital Tübingen) was
537 added to a final concentration of 5% and bacteria were opsonized for 10 min at 37°C, as described

538 recently (Peschel et al., 2001). Prewarmed bacteria and PMNs were mixed to final concentrations of
539 5×10^6 CFU/ml and 2.5×10^6 PMNs/ml in flat-bottom 96 well plates together with antibodies (final
540 concentration 100 µg/ml). Samples of 50 µl were shaken at 37°C.

541 For analysis of the PMN killing capacity, incubation was stopped at different time points by the
542 addition of 100-fold volumes of ice-cold distilled water to disrupt the PMNs. Triplets of appropriate
543 sample volumes were spread on LB agar plates and colonies were counted after 24 h incubation at
544 37°C. Numbers of live bacteria did not change during the 60-min incubation period in the absence of
545 PMNs compared to the initial bacteria counts.

546 For phagocytosis studies, overnight cultures of bacteria were labeled with 0.1 mg/ml fluorescein-5-
547 isothiocyanate (FITC) at 37°C for 1 h, as described previously (Peschel et al., 2001). After washing
548 with PBS, the bacteria were resuspended in HBSS-HSA, adjusted to 5×10^6 CFU/ml, mixed with PMNs
549 (2.5×10^6 PMNs/ml), and opsonized as described above (shaking at 37°C). Incubation was stopped by
550 addition of 100 µl ice-cold 1% paraformaldehyde. The percentage of PMNs bearing FITC-labeled
551 bacteria was determined by flow cytometric analysis of 20,000 cells.

552

553 ***Murine CA-MRSA skin abscess infection model***

554 Male Swiss-Webster mice (5-6 weeks old) were obtained from Harlan Sprague-Dawley, Inc. Mice
555 were housed at four animals per cage. Food and water were provided to the mice ad libitum. CA-
556 MRSA strain USA300 was grown in the presence of antibodies (100 µg/ml) as described above for
557 determination of susceptibility to antimicrobials, and bacteria were suspended in PBS. Bacterial
558 suspensions were mixed with equal volumes of dextran bead solution (Cytodex-1 microcarriers;
559 Sigma-Aldrich) and antibodies at final concentration of 100 µg/ml, and adjusted to a final bacterial
560 load of 10^6 CFU in 0.2 ml PBS / dextran beads (1:1). Groups of four mice per antibody were injected
561 subcutaneously in each flank with 0.2 ml of *S. aureus* suspensions. The numbers of CFU per milliliter
562 of inoculum were verified by plate counts. 36 hours after abscess induction, mice were euthanized

563 and abscesses were excised and homogenized in 1 ml of PBS. Serial dilutions of the homogenates
564 were plated in triplicates on tryptic soy agar plates.

565

566 ***Study approval***

567 Animal experiments were performed in strict accordance with the German regulations of the Society
568 for Laboratory Animal Science (GV-SOLAS) and the European Health Law of the Federation of
569 Laboratory Animal Science Associations (FELASA). The protocol was approved by the
570 Regierungspräsidium Tübingen (permit no. H2/10).

571

572 **Statistics**

573 Statistical analyses were performed with the Prism 5.0 package (GraphPad Software) and Group
574 differences were analyzed for significance with the two-tailed Student's *t* test. A *P* value of ≤0.05 was
575 considered statistically significant.

576

577 **Author contributions**

578 C.J.S, A.K., S.W., M.T., C.W., B.K., C.M.E., and A.P. conceived and designed the experiments. C.J.S. (all
579 methods), J.N.H. (SCAM), C.G. (antimicrobial agent susceptibility analysis), J.S. (skin abscess model),
580 A.G. (SCAM), D.H. (antigen selection and antibody production, ELISAs, growth curves), B.K. (cloning
581 and mutagenesis), and C.M.E. (cloning and mutagenesis, antimicrobial agent susceptibility testing)
582 performed the experiments. C.J.S., J.N.H., J.S., A.G., A.K., S.W., S.K., C.M.E., and A.P. analyzed the
583 data. S.W., M.T., C.W., and A.P. contributed material / analysis tools. C.J.S., J.N.H., S.W., C.M.E., and
584 A.P. wrote the paper.

585

Acknowledgements

This work was financed by Grants from the German Research Foundation TRR34, SFB766, TRR156, TRR261, and GRK1708 to A.P.; and the German Center of Infection Research (DZIF) to A.P. C.J.S. was supported by the intramural Experimental Medicine program of the Medical Faculty at the University of Tübingen and received grants from the DZIF and the cluster of Excellence EXC2124 Controlling Microbes to Fight Infection (CMFI). The authors acknowledge infrastructural support by the cluster of Excellence EXC2124 CMFI.

Figures

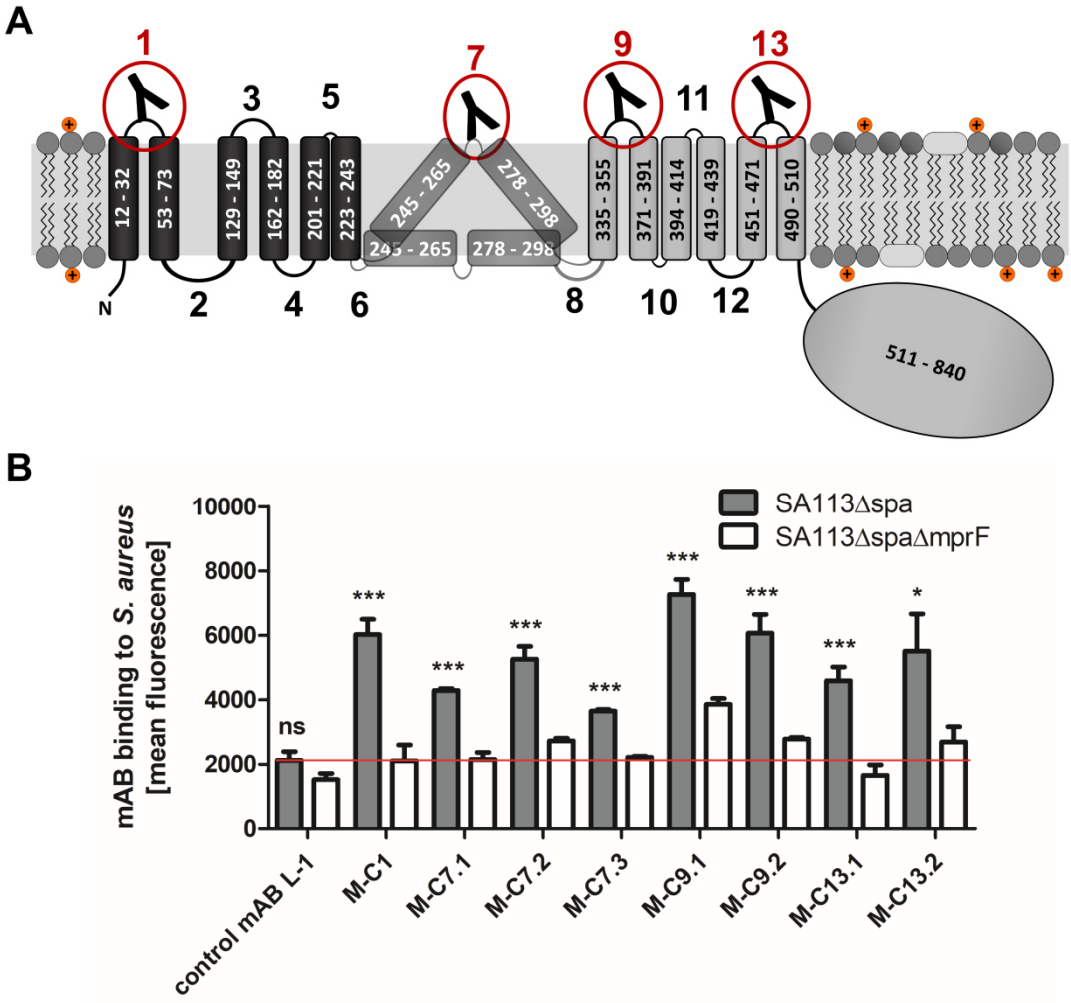

597 **Figure 1.** MprF topology and binding of mABs to targeted MprF-expressing *S. aureus* cells. (A) MprF
598 membrane topology is given according to our recent study (Ernst et al., 2015) showing synthase and
599 flippase domains in gray and black, respectively. Amino acid (aa) positions of TMS and the C-terminal
600 hydrophilic domain are indicated. TMSs from aa 245-265 and aa 278-298 are shown transparently as
601 computational and experimental results of transmembrane topology were contradictory (Ernst et al.,
602 2015). Localizations of MprF's TMS-connecting loops are numbered starting from the N-terminus,
603 antibody targeted loops are indicated by red circles and antibody symbols. (B) Specific binding of
604 mABs (100 nM) to *S. aureus* SA113 WT and *ΔmprF* analyzed by ELISA. Both, SA113 WT and *ΔmprF*
605 were deficient in the IgG-binding protein A (Spa). The red line indicates the mean fluorescence
606 measured at A 440 nm (affinity) of the control mAB L-1 bound to *S. aureus* SA113*Δspa.* Means and
607 SEM of at least three experiments are shown. Significant differences between WT and *ΔmprF* were
608 calculated by Student's paired t-test (ns, not significant; *, $P < 0.05$; ***, $P < 0.0001$).

609

610

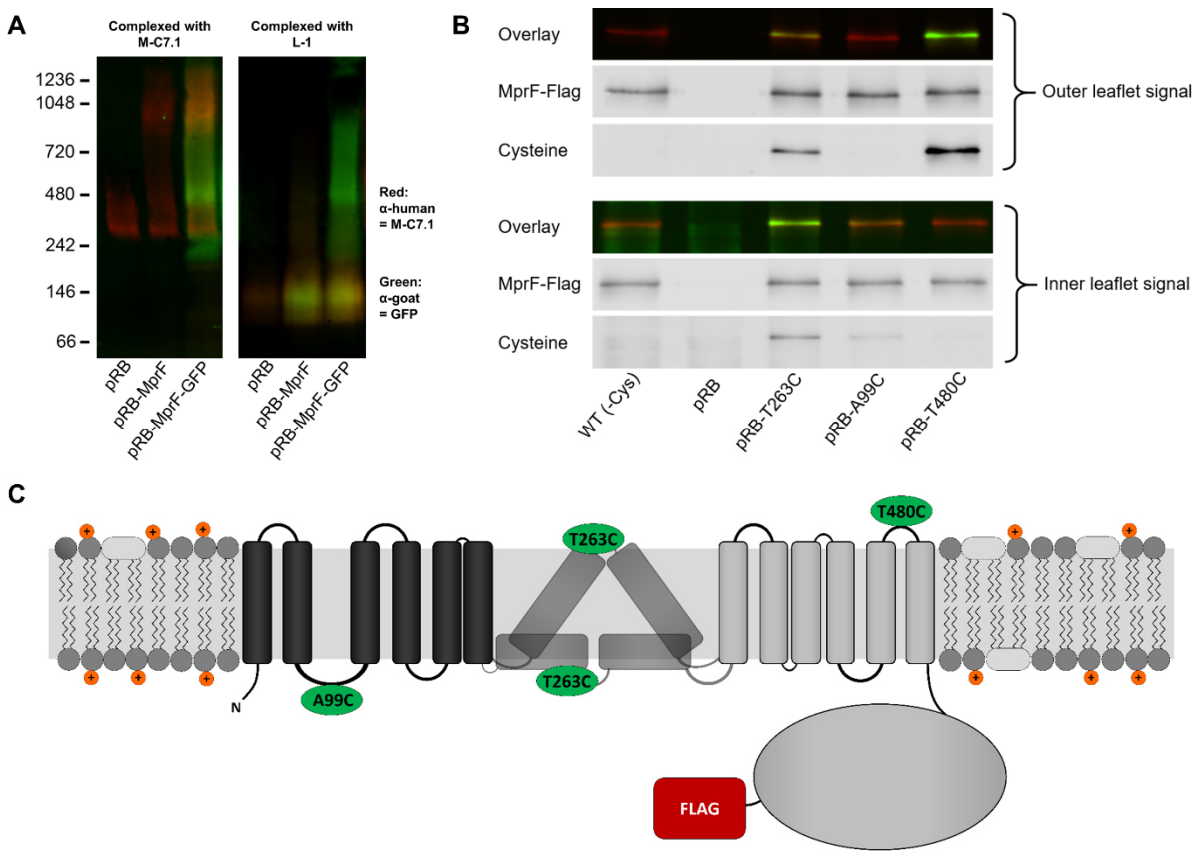

611

612 **Figure 2.** Binding of M-C7.1 to MprF and membrane localization of the M-C7.1-targeted MprF loop
613 seven. (A) Detection of M-C7.1 binding to MprF. Plasmid-encoded native and GFP-tagged MprF
614 variants were expressed in *S. aureus* SA113*ΔspaΔmprF* and living cells were preincubated with M-
615 C7.1 or the control mAB L-1 (in order to form MprF-mAB complexes). MprF variants/complexes were
616 detected by blue native Western blotting via primary (anti-GFP and M-C7.1) and secondary
617 antibodies (red for secondary antibody detection of M-C7.1; green for secondary antibody detection
618 of anti-GFP). SA113*ΔspaΔmprF* expressing the empty vector (pRB) served as negative control.
619 Molecular masses in kDa of marker proteins are given on the left of the gel. (B) Cellular localization of
620 the antigen epitope of M-C7.1 using the substituted cysteine accessibility method (SCAM) for specific
621 loops between the MprF TMSs. The substituted cysteine T263C is localized in M-C7.1´s target peptide
622 sequence in MprF. Substitution of A99C served as inside control, substitution of T480C served as
623 outside control (see topology model, part C). *S. aureus* SA113*ΔmprF* expressing the empty vector
624 (pRB) and an MprF variant lacking all native cysteines (WT (-Cys)) served as additional negative
625 controls. All MprF variants were plasmid-encoded, FLAG®-tagged at the C-terminus to allow
626 immunoprecipitation and detection, and were expressed in *S. aureus* SA113*ΔmprF*. Substituted
627 extracellular cysteine residues were labeled with Na*-(3-maleimidylpropionyl)-biocytin (MPB) (outer
628 leaflet signal, green in overlay), while labeling of substituted internal cysteine with MPB was
629 performed after the blocking of external cysteines with 4-acetamino-4'-maleimidylstilbene-2,2'-
630 disulfonic acid (AMS) (inner leaflet signal, green in overlay). MprF was detected via antibody staining
631 by an anti-FLAG® antibody (red in overlay). (C) MprF topology showing location and amino acid
632 exchanges of artificial cysteine residues for SCAM detection in green.

633

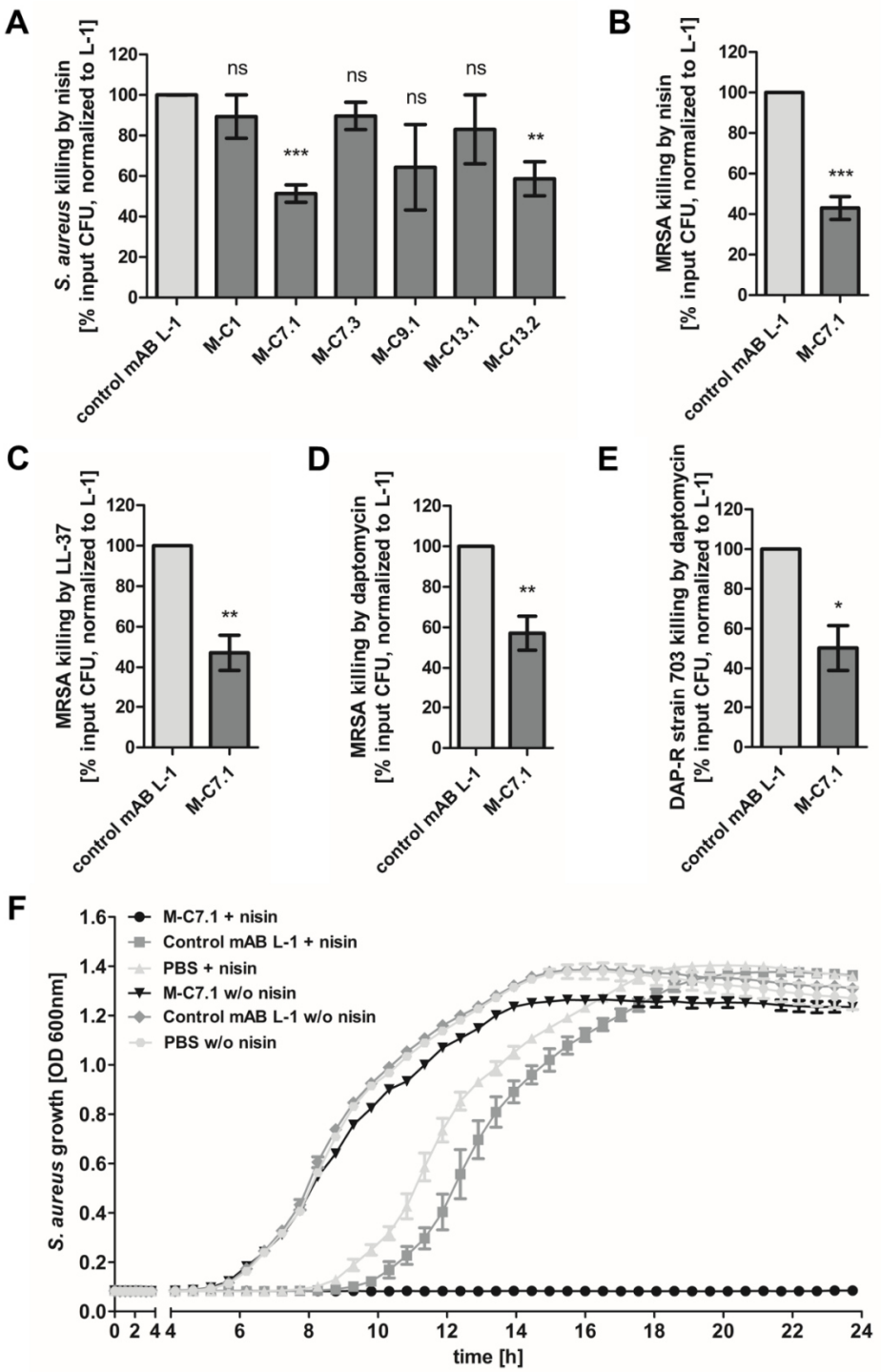

634

635 **Figure 3.** Killing and growth inhibition of *S. aureus* by antimicrobial peptides and antibiotics in the
636 presence of M-C7.1. (A) Survival of *S. aureus* SA113*Δspa* in the presence of nisin and anti-MprF
637 antibodies compared to control mAB L-1. Surviving CFU of each antibody (and nisin) containing
638 sample were analyzed after 3 h incubation and the negative control (mAB L-1) was set to 100 %
639 survival. (B) Survival of CA-MRSA strain USA300 in the presence of nisin and M-C7.1 compared to the
640 control mAB L-1. (C) Survival of USA300 in the presence of LL-37 and M-C7.1 compared to the control

641 mAB L-1. (D) Survival of USA300 in the presence of daptomycin and M-C7.1 compared to the control
642 mAB L-1. (E) Survival of daptomycin-resistant CA-MRSA strain 703 (Jones et al., 2008) in the presence
643 of daptomycin and M-C7.1 compared to the control mAB L-1. (F) Growth inhibition of USA300 in the
644 presence of subinhibitory nisin concentrations and M-C7.1 compared to the control mAB L-1. Wells
645 without nisin and/or antibodies served as additional negative controls. The means plus SEM of
646 results from at least three independent experiments are shown in A-E. Technical duplicates were
647 employed for each analysis. F shows means plus SEM of technical triplicates from a representative
648 experiment of three independent experiments. Values for M-C7.1 or other anti-MprF antibodies that
649 were significantly different from those for the control mAB L-1, calculated by Student's paired t-test
650 are indicated (*, $P < 0.05$; **, $P < 0.01$; ***, $P < 0.0001$).

651

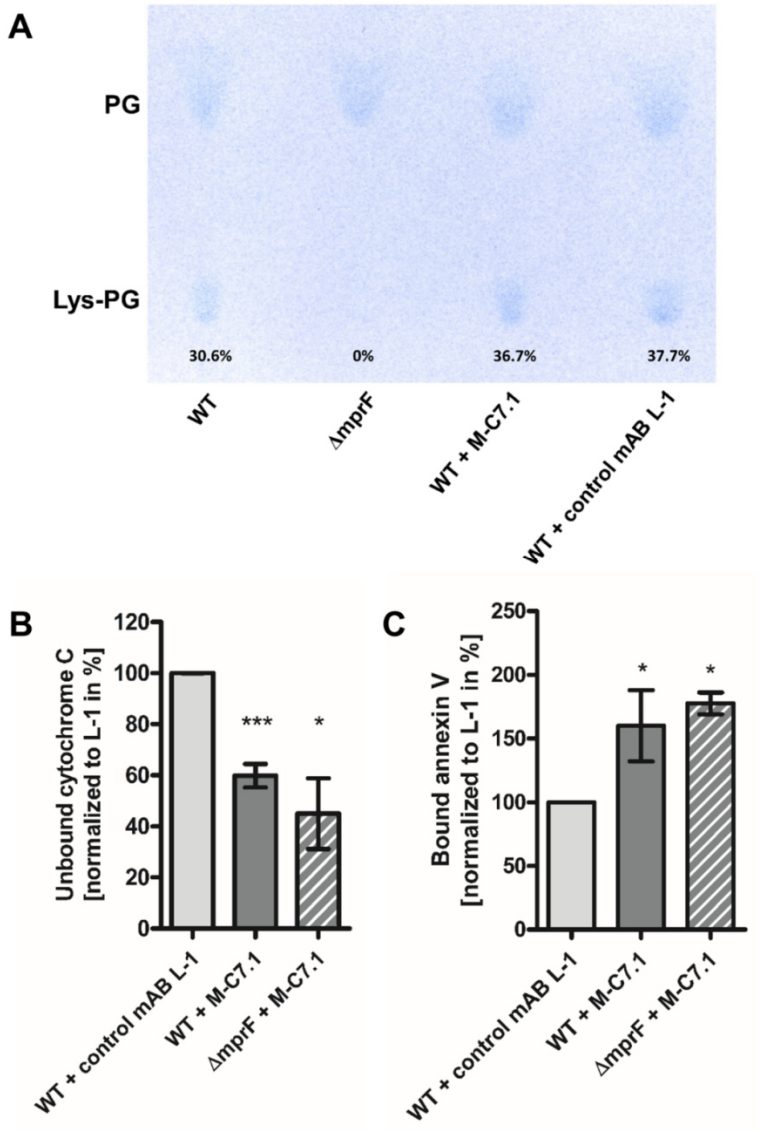

Figure 4. M-C7.1 inhibits the MprF LysPG flippase but not the LysPG synthase. (A) Detection of phospholipids from *S. aureus* SA113*ΔmprF* and WT treated or not treated with M-C7.1 or the control mAB L-1. Polar lipids were separated by TLC and stained with the phosphate group-specific dye molybdenum blue to detect the well-documented PG and LysPG pattern of *S. aureus* WT and *mprF* deletion mutant (Slavetinsky et al., 2012). Percentages of LysPG in relation to total phospholipid content are given below respective LysPG spots. (B) The repulsion of positively charged cytochrome C corresponds to MprF LysPG synthase plus flippase activity while the synthase activity alone does not affect repulsion. To assess MprF flippase efficiency, unbound cytochrome C in the supernatant was quantified photometrically after incubation with the *S. aureus* SA113 WT pretreated with M-C7.1 or the control mAB L-1 (the latter set to 100%). SA113*ΔmprF* treated with M-C7.1 served as negative

663 control. The means plus SEM of results from three independent experiments are shown. (C) Annexin
664 V binding to *S. aureus* SA113 WT after incubation with M-C7.1 or the control mAB L-1 was quantified
665 by measuring cell-bound annexin V by FACS and L-1 treated samples were set to 100%. Data are
666 expressed in relative fluorescence units. The means plus SEM of results from three independent
667 experiments are shown in B and C. Significant differences between M-C7.1 and L-1-treated samples
668 were calculated by Student's paired t-test (*, $P < 0.05$; ***, $P < 0.0001$).

669

670

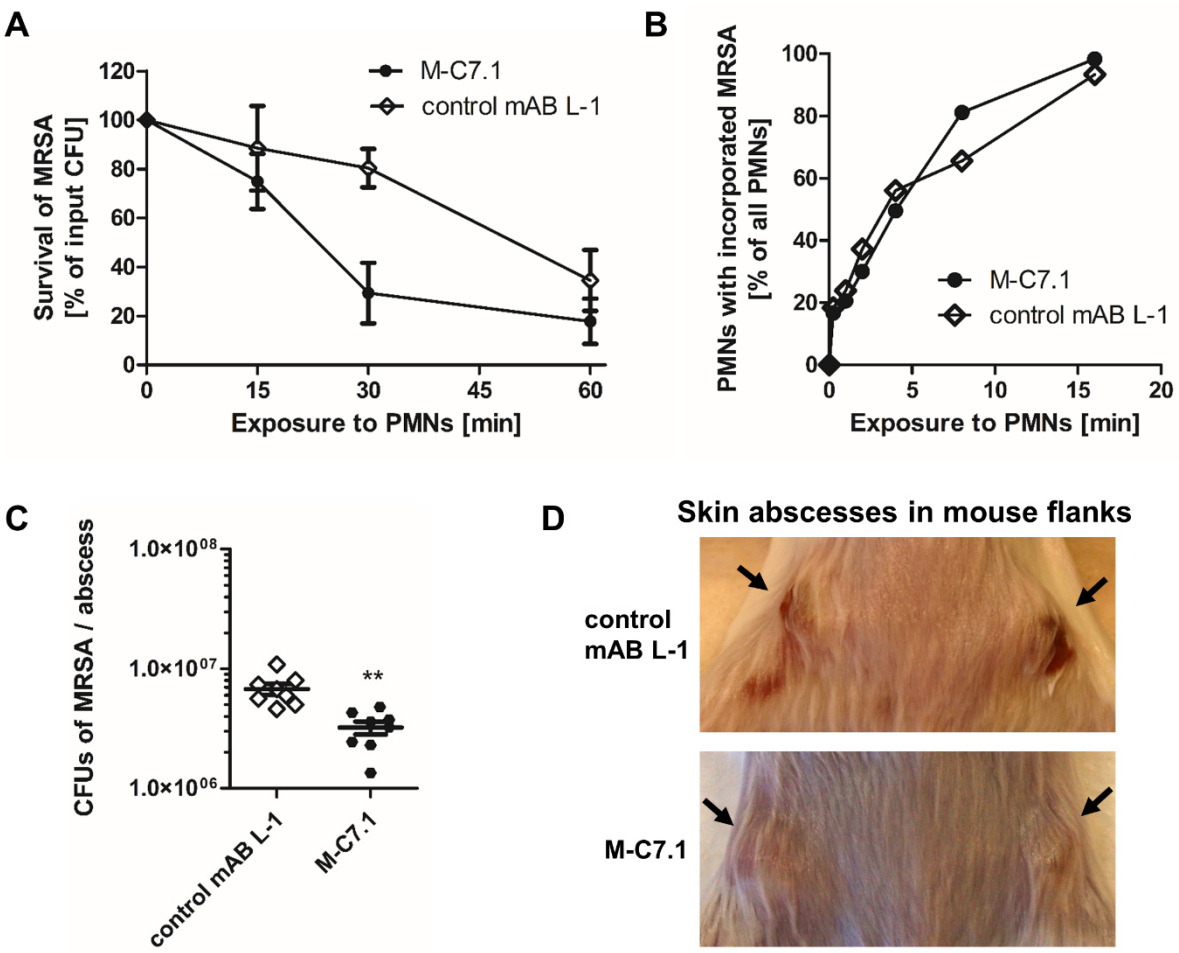

671

672 **Figure 5.** M-C7.1 supports *S. aureus* clearance by isolated human PMNs and in an *in vivo* abscess
673 model. (A) Kinetics of killing of CA-MRSA strain USA300 WT treated with M-C7.1 compared to control
674 mAB L-1 by freshly isolated human PMNs. Viable bacteria (CFU) after incubation with PMNs are
675 shown as percentage of initial CFU counts. The means plus SEM of results from three independent

676 experiments are shown. (B) Kinetics of phagocytosis of USA300 WT treated with M-C7.1 compared to
677 control mAB L-1 by freshly isolated human PMNs. Percentages of PMNs bearing FITC-labeled USA300
678 are given. Means of three counts from a representative experiment are shown. (C) Skin abscess
679 formation by USA300 WT treated with M-C7.1 compared to control mAB L-1 in mice. Abscesses were
680 induced by 10^6 CFUs of antibody-treated bacterial cells mixed with dextran beads (1:1) and injected
681 s.c. in both flanks of mice. Mice were euthanized after 36 h, abscesses were excised and viable
682 bacteria in homogenized samples were quantified. Eight abscesses from four mice per antibody are
683 shown together with medians. Significant differences were calculated by Student's t-test (**,
684 $P < 0.01$) (D) Visual phenotype of two representative skin abscesses induced by M-C7.1 or control
685 mAB L-1 treated USA300 WT in the flanks of mice. Abscesses are indicated by black arrows.

686

687

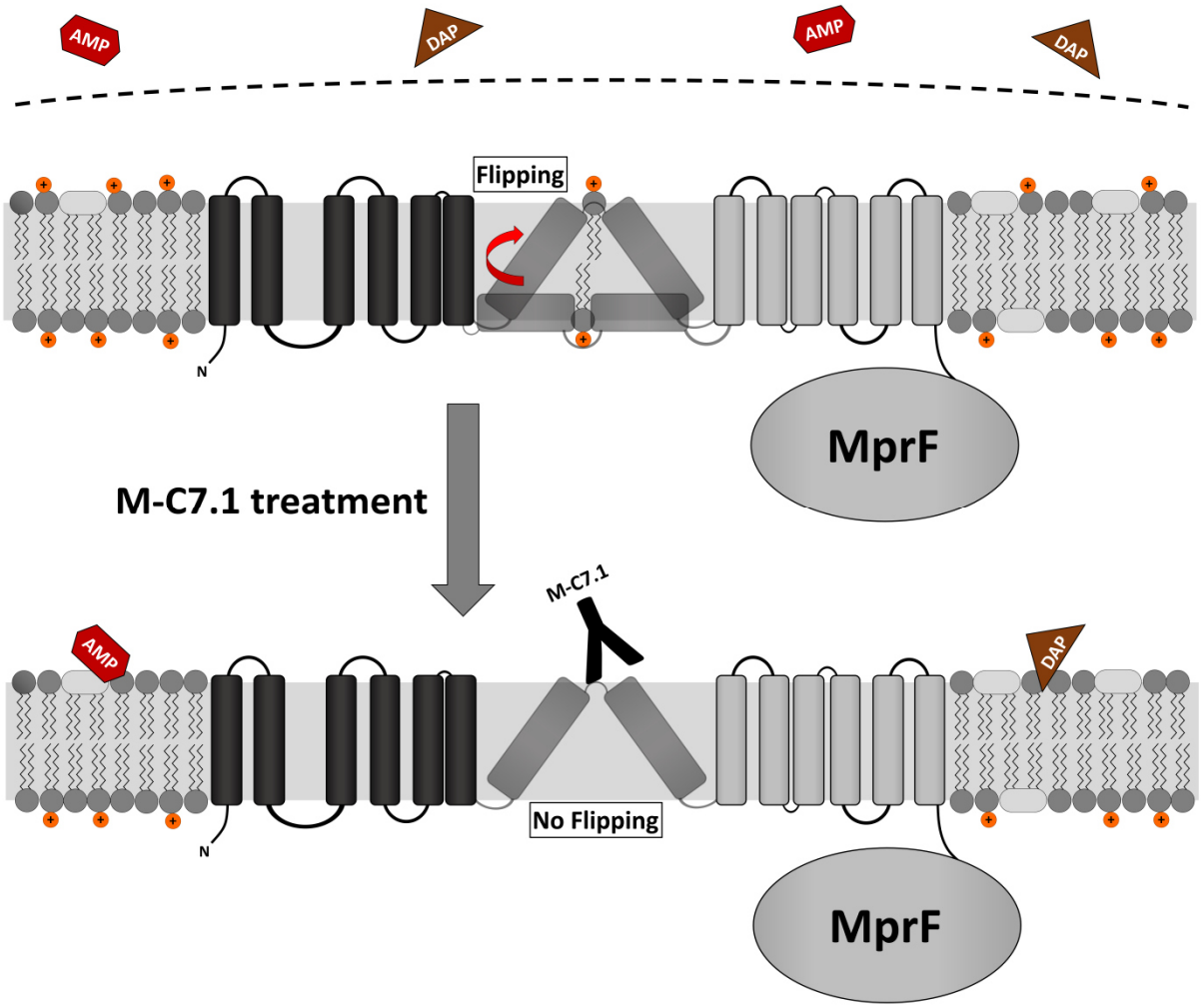

688

689 **Figure 6.** Proposed model for MprF inhibition by M-C7.1. Flipping of positively charged LysPG
690 probably by TMS 7 and 8 of MprF results in a more positively charged staphylococcal membrane able
691 to repulse AMPs or daptomycin (DAP). Binding of M-C7.1 to MprF loop seven blocks the flippase
692 which results in a more negatively charged staphylococcal membrane and subsequently in an
693 increased *S. aureus* membrane disruption by AMPs and daptomycin.

694

695 **References**

696 Ardal C, Balasegaram M, Laxminarayan R, McAdams D, Outterson K, Rex JH, Sumpradit N (2020)
697 Antibiotic development - economic, regulatory and societal challenges. *Nat Rev Microbiol* 18: 267-
698 274
699 Bae T, Schneewind O (2006) Allelic replacement in Staphylococcus aureus with inducible counter-
700 selection. *Plasmid* 55: 58-63
701 Bayer AS, Schneider T, Sahl HG (2013) Mechanisms of daptomycin resistance in Staphylococcus
702 aureus: role of the cell membrane and cell wall. *Ann N Y Acad Sci* 1277: 139-58
703 Bligh EG, Dyer WJ (1959) A rapid method of total lipid extraction and purification. *Can J Biochem*
704 *Physiol* 37: 911-7
705 Bogdanov M, Zhang W, Xie J, Dowhan W (2005) Transmembrane protein topology mapping by the
706 substituted cysteine accessibility method (SCAM(TM)): application to lipid-specific membrane protein
707 topogenesis. *Methods* 36: 148-71
708 Bruckner R (1992) A series of shuttle vectors for Bacillus subtilis and Escherichia coli. *Gene* 122: 187-
709 92
710 Chen Z, Moayeri M, Purcell R (2011) Monoclonal antibody therapies against anthrax. *Toxins (Basel)* 3:
711 1004-19
712 Denis K, Le Bris M, Le Guennec L, Barnier JP, Faure C, Gouge A, Bouzinba-Segard H, Jamet A,
713 Euphrasie D, Durel B, Barois N, Pelissier P, Morand PC, Coureuil M, Lafont F, Join-Lambert O, Nassif X,
714 Bourdoulous S (2019) Targeting Type IV pili as an antivirulence strategy against invasive
715 meningococcal disease. *Nat Microbiol* 4: 972-984
716 Dickey SW, Cheung GYC, Otto M (2017) Different drugs for bad bugs: antivirulence strategies in the
717 age of antibiotic resistance. *Nat Rev Drug Discov* 16: 457-471
718 Ernst CM, Kuhn S, Slavetinsky CJ, Krismer B, Heilbronner S, Gekeler C, Kraus D, Wagner S, Peschel A
719 (2015) The lipid-modifying multiple peptide resistance factor is an oligomer consisting of distinct
720 interacting synthase and flippase subunits. *MBio* 6
721 Ernst CM, Peschel A (2011) Broad-spectrum antimicrobial peptide resistance by MprF-mediated
722 aminoacylation and flipping of phospholipids. *Mol Microbiol* 80: 290-9
723 Ernst CM, Slavetinsky CJ, Kuhn S, Hauser JN, Nega M, Mishra NN, Gekeler C, Bayer AS, Peschel A
724 (2018) Gain-of-Function Mutations in the Phospholipid Flippase MprF Confer Specific Daptomycin
725 Resistance. *MBio* 9
726 Ernst CM, Staubitz P, Mishra NN, Yang SJ, Hornig G, Kalbacher H, Bayer AS, Kraus D, Peschel A (2009)
727 The bacterial defensin resistance protein MprF consists of separable domains for lipid lysinylation
728 and antimicrobial peptide repulsion. *PLoS Pathog* 5: e1000660
729 Hanzelmann D, Joo HS, Franz-Wachtel M, Hertlein T, Stevanovic S, Macek B, Wolz C, Gotz F, Otto M,
730 Kretschmer D, Peschel A (2016) Toll-like receptor 2 activation depends on lipopeptide shedding by
731 bacterial surfactants. *Nat Commun* 7: 12304
732 Ieronymaki M, Nuti F, Brancaccio D, Rossi G, Real-Fernandez F, Cao Y, Monasson O, Larregola M,
733 Peroni E, Uziel J, Sabatino G, Novellino E, Carotenuto A, Papini AM, Rovero P (2017) Structure-Activity
734 Relationship Studies, SPR Affinity Characterization, and Conformational Analysis of Peptides That
735 Mimic the HNK-1 Carbohydrate Epitope. *ChemMedChem* 12: 751-759
736 Iordanescu S, Surdeanu M (1976) Two restriction and modification systems in Staphylococcus aureus
737 NCTC8325. *J Gen Microbiol* 96: 277-81
738 Jones T, Yeaman MR, Sakoulas G, Yang SJ, Proctor RA, Sahl HG, Schrenzel J, Xiong YQ, Bayer AS (2008)
739 Failures in clinical treatment of Staphylococcus aureus Infection with daptomycin are associated with
740 alterations in surface charge, membrane phospholipid asymmetry, and drug binding. *Antimicrob*
741 *Agents Chemother* 52: 269-78
742 Kim HK, Thammavongsa V, Schneewind O, Missiakas D (2012) Recurrent infections and immune
743 evasion strategies of Staphylococcus aureus. *Curr Opin Microbiol* 15: 92-9

744 Kristian SA, Durr M, Van Strijp JA, Neumeister B, Peschel A (2003) MprF-mediated lysinylation of
745 phospholipids in Staphylococcus aureus leads to protection against oxygen-independent neutrophil
746 killing. *Infect Immun* 71: 546-9
747 Lakemeyer M, Zhao W, Mandl FA, Hammann P, Sieber SA (2018) Thinking Outside the Box-Novel
748 Antibacterials To Tackle the Resistance Crisis. *Angew Chem Int Ed Engl* 57: 14440-14475
749 Lee AS, de Lencastre H, Garau J, Kluytmans J, Malhotra-Kumar S, Peschel A, Harbarth S (2018)
750 Methicillin-resistant Staphylococcus aureus. *Nat Rev Dis Primers* 4: 18033
751 Missiakas D, Schneewind O (2016) Staphylococcus aureus vaccines: Deviating from the carol. *J Exp*
752 *Med* 213: 1645-53
753 Neuber T, Frese K, Jaehrling J, Jager S, Daubert D, Felderer K, Linnemann M, Hohne A, Kaden S, Kolln
754 J, Tiller T, Brocks B, Ostendorp R, Pabst S (2014) Characterization and screening of IgG binding to the
755 neonatal Fc receptor. *MAbs* 6: 928-42
756 Otto M (2013) Community-associated MRSA: what makes them special? *Int J Med Microbiol* 303:
757 324-30
758 Peschel A, Jack RW, Otto M, Collins LV, Staubitz P, Nicholson G, Kalbacher H, Nieuwenhuizen WF,
759 Jung G, Tarkowski A, van Kessel KP, van Strijp JA (2001) Staphylococcus aureus resistance to human
760 defensins and evasion of neutrophil killing via the novel virulence factor MprF is based on
761 modification of membrane lipids with l-lysine. *J Exp Med* 193: 1067-76
762 Peschel A, Otto M, Jack RW, Kalbacher H, Jung G, Gotz F (1999) Inactivation of the dlt operon in
763 Staphylococcus aureus confers sensitivity to defensins, protegrins, and other antimicrobial peptides.
764 *J Biol Chem* 274: 8405-10
765 Pinheiro da Silva F, Machado MC (2017) The dual role of cathelicidins in systemic inflammation.
766 *Immunol Lett* 182: 57-60
767 Posteraro B, Pea F, Masucci L, Posteraro P, Sanguinetti M (2018) Actoxumab + bezlotoxumab
768 combination: what promise for Clostridium difficile treatment? *Expert Opin Biol Ther* 18: 469-476
769 Prassler J, Thiel S, Pracht C, Polzer A, Peters S, Bauer M, Norenberg S, Stark Y, Kolln J, Popp A,
770 Urlinger S, Enzelberger M (2011) HuCAL PLATINUM, a synthetic Fab library optimized for sequence
771 diversity and superior performance in mammalian expression systems. *J Mol Biol* 413: 261-78
772 Qu X, Tang Y, Hua S (2018) Immunological Approaches Towards Cancer and Inflammation: A Cross
773 Talk. *Front Immunol* 9: 563
774 Roy H, Ibba M (2009) Broad range amino acid specificity of RNA-dependent lipid remodeling by
775 multiple peptide resistance factors. *J Biol Chem* 284: 29677-83
776 Slavetinsky C, Kuhn S, Peschel A (2016) Bacterial aminoacyl phospholipids - Biosynthesis and role in
777 basic cellular processes and pathogenicity. *Biochim Biophys Acta*
778 Slavetinsky CJ, Peschel A, Ernst CM (2012) Alanyl-phosphatidylglycerol and lysyl-phosphatidylglycerol
779 are translocated by the same MprF flippases and have similar capacities to protect against the
780 antibiotic daptomycin in Staphylococcus aureus. *Antimicrob Agents Chemother* 56: 3492-7
781 Spaan AN, Surewaard BG, Nijland R, van Strijp JA (2013) Neutrophils versus Staphylococcus aureus: a
782 biological tug of war. *Annu Rev Microbiol* 67: 629-50
783 Tabor DE, Yu L, Mok H, Tkaczyk C, Sellman BR, Wu Y, Oganesyan V, Slidel T, Jafri H, McCarthy M,
784 Bradford P, Esser MT (2016) Staphylococcus aureus Alpha-Toxin Is Conserved among Diverse Hospital
785 Respiratory Isolates Collected from a Global Surveillance Study and Is Neutralized by Monoclonal
786 Antibody MEDI4893. *Antimicrob Agents Chemother* 60: 5312-21
787 Tacconelli E, Carrara E, Savoldi A, Harbarth S, Mendelson M, Monnet DL, Pulcini C, Kahlmeter G,
788 Kluytmans J, Carmeli Y, Ouellette M, Outterson K, Patel J, Cavaleri M, Cox EM, Houchens CR, Grayson
789 ML, Hansen P, Singh N, Theuretzbacher U et al. (2017) Discovery, research, and development of new
790 antibiotics: the WHO priority list of antibiotic-resistant bacteria and tuberculosis. *Lancet Infect Dis*
791 Theuretzbacher U, Outterson K, Engel A, Karlen A (2019) The global preclinical antibacterial pipeline.
792 *Nat Rev Microbiol*
793 Tiller T, Schuster I, Deppe D, Siegers K, Strohner R, Herrmann T, Berenguer M, Poujol D, Stehle J,
794 Stark Y, Hessling M, Daubert D, Felderer K, Kaden S, Kolln J, Enzelberger M, Urlinger S (2013) A fully

795 synthetic human Fab antibody library based on fixed VH/VL framework pairings with favorable
796 biophysical properties. *MAbs* 5: 445-70
797 Wang R, Braughton KR, Kretschmer D, Bach TH, Queck SY, Li M, Kennedy AD, Dorward DW, Klebanoff
798 SJ, Peschel A, DeLeo FR, Otto M (2007) Identification of novel cytolytic peptides as key virulence
799 determinants for community-associated MRSA. *Nat Med* 13: 1510-4
800 Yount NY, Kupferwasser D, Spisni A, Dutz SM, Ramjan ZH, Sharma S, Waring AJ, Yeaman MR (2009)
801 Selective reciprocity in antimicrobial activity versus cytotoxicity of hBD-2 and crotamine. *Proc Natl*
802 *Acad Sci U S A* 106: 14972-7
803 Zheng Y, Shang W, Peng H, Rao Y, Zhao X, Hu Z, Yang Y, Hu Q, Tan L, Xiong K, Li S, Zhu J, Hu X, Zhou R,
804 Li M, Rao X (2019) Virulence Determinants Are Required for Brain Abscess Formation Through
805 Staphylococcus aureus Infection and Are Potential Targets of Antivirulence Factor Therapy. *Front*
806 *Microbiol* 10: 682

807

808

809 **Supplemental figures**

810

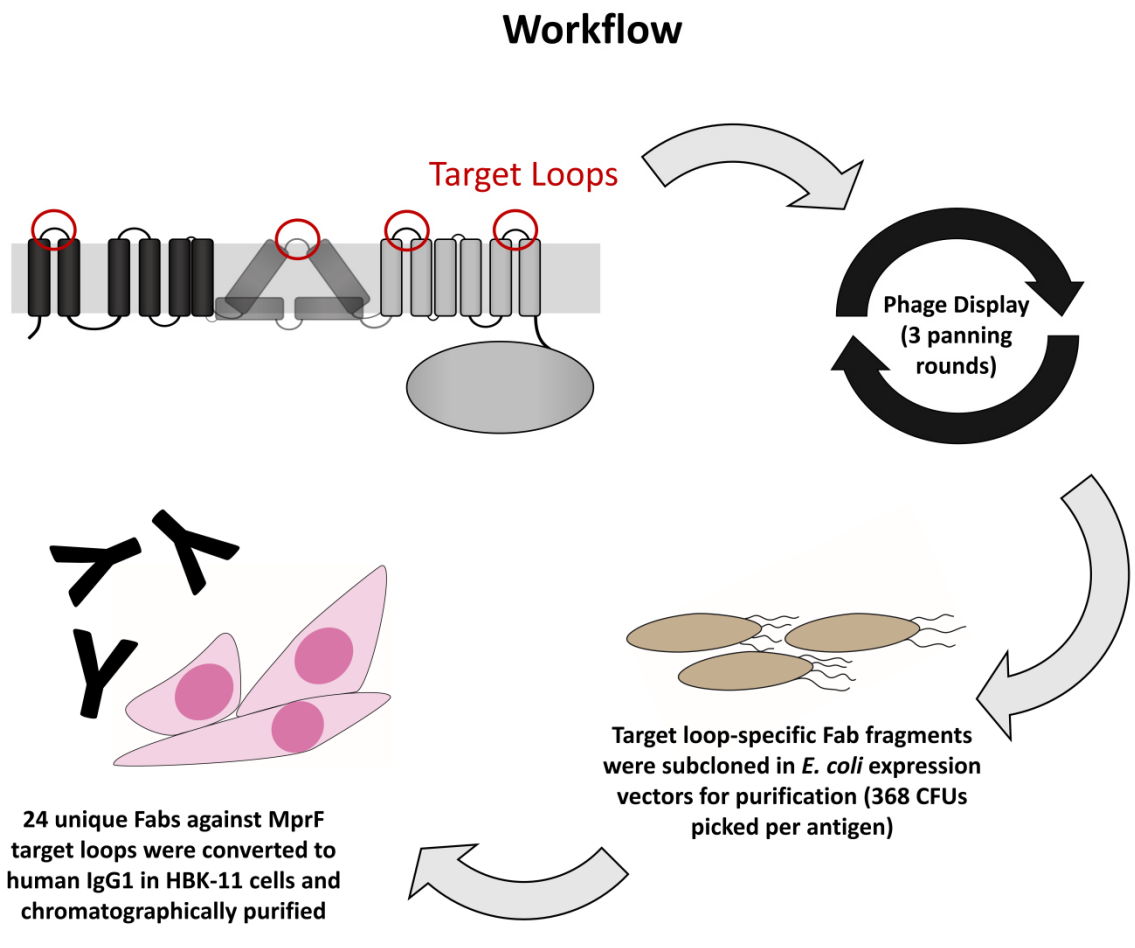

811

812 **Supplemental Figure S1.** Workflow for the development of MprF specific mABs. Biotinylated MprF

813 peptide loops were incubated with the HuCal phage display library expressing single-chain human

814 Fab fragments, antigen-binding phages were enriched in three iterative panning rounds, bound

815 antigen-specific phages were isolated and subcloned in *E. coli* expression vectors to yield His-tagged

816 Fab fragments, 24 unique Fabs against all peptides were converted to human IgG by cloning in an

817 IgG1 expression vector system for human HKB11 cells, and IgGs were purified via protein A

818 chromatography.

819

820

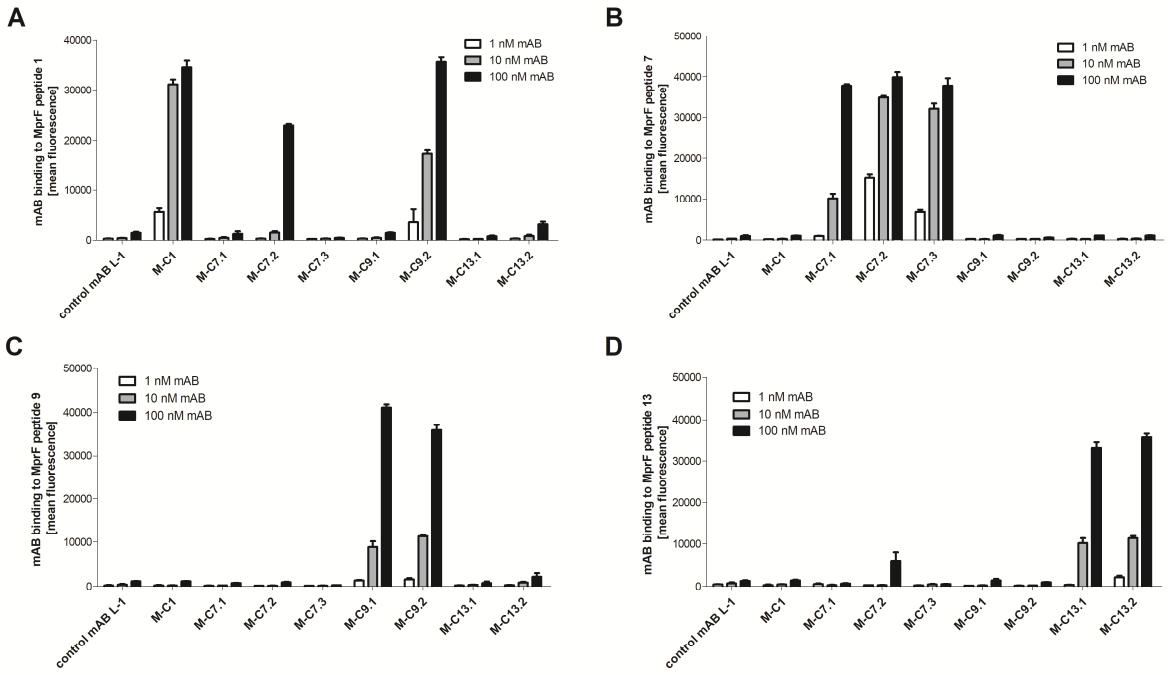

821

822 **Supplemental Figure S2.** Specific binding of selected mABs to cyclic MprF-derived target peptides
823 was analyzed by ELISA. Biotinylated cyclic peptides corresponding to the MprF loops 1, 7, 9, and 13
824 were incubated with eight anti-MprF IgGs in PBS compared to the control mAB L-1. (A-D) show
825 binding of mABs at increasing concentrations to cyclic MprF loops 1, 7, 9, and 13, respectively. Mean
826 fluorescence measured at A 440 nm and SEM of three independent experiments are shown.

827

828

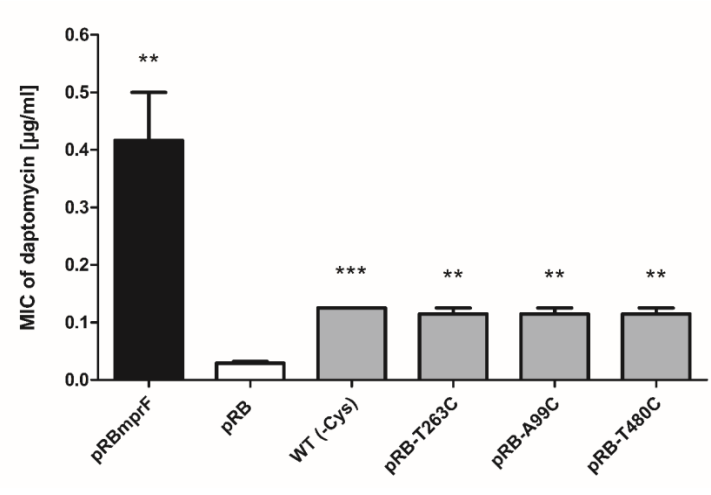

829

830 **Supplemental Figure S3.** Effects of cysteine replacement and insertion on MprF function, assessed by
831 measuring daptomycin susceptibility. Minimal inhibitory concentrations (MICs) of daptomycin

832 against the indicated *S. aureus* strains are shown. The *mprF* deletion mutant with empty pRB474
833 plasmid served as a negative control. The means plus SEM of results from three independent
834 experiments are shown. Values that are significantly different from the values determined for the *S.*
835 *aureus ΔmprF* mutant bearing pRB474 (pRB), calculated by Student´s paired t-test, are indicated (**,
836 $P < 0.01$; ***, $P < 0.0001$).

837

838

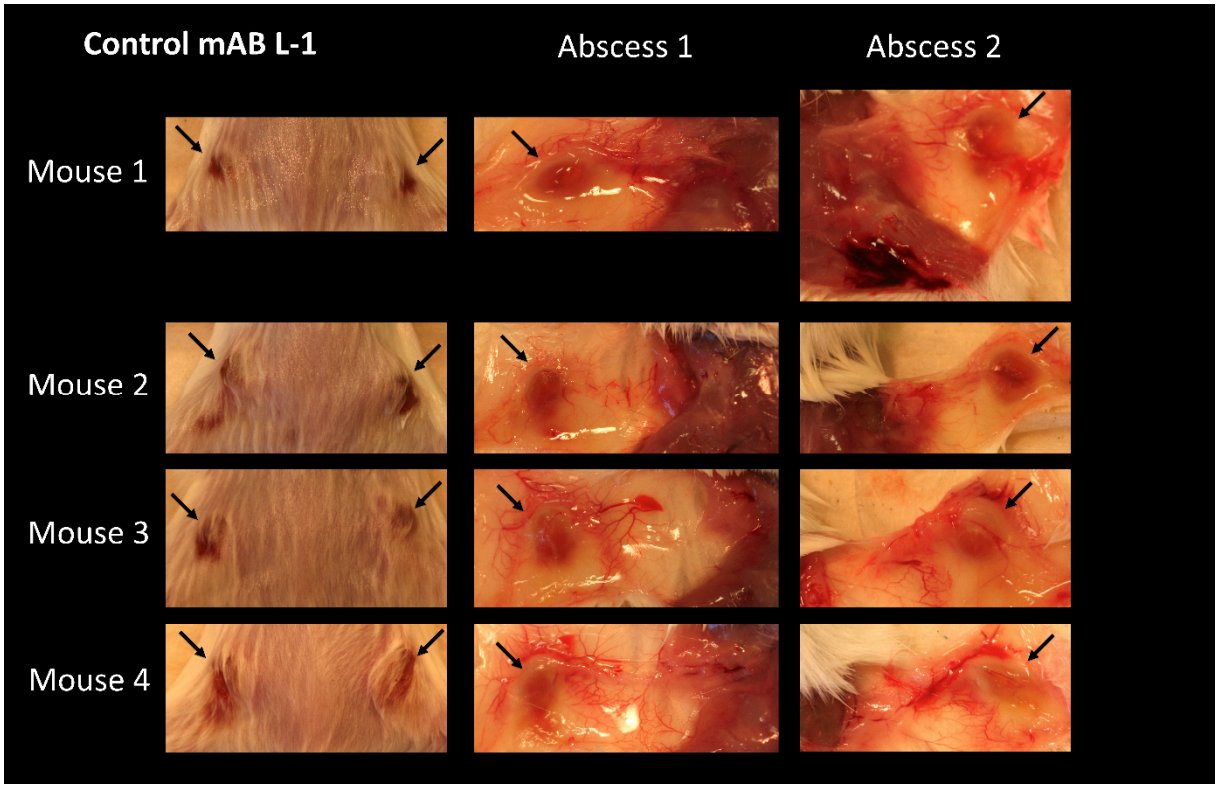

839

840 **Supplemental Figure S4A**. Visual phenotypes of all mouse skin abscesses caused by USA300 WT
841 treated with the control mAB L-1. Abscesses indicated by black arrows, abscess 1 represents the
842 opened right abscess, abscess 2 represents the opened left abscess.

843

844

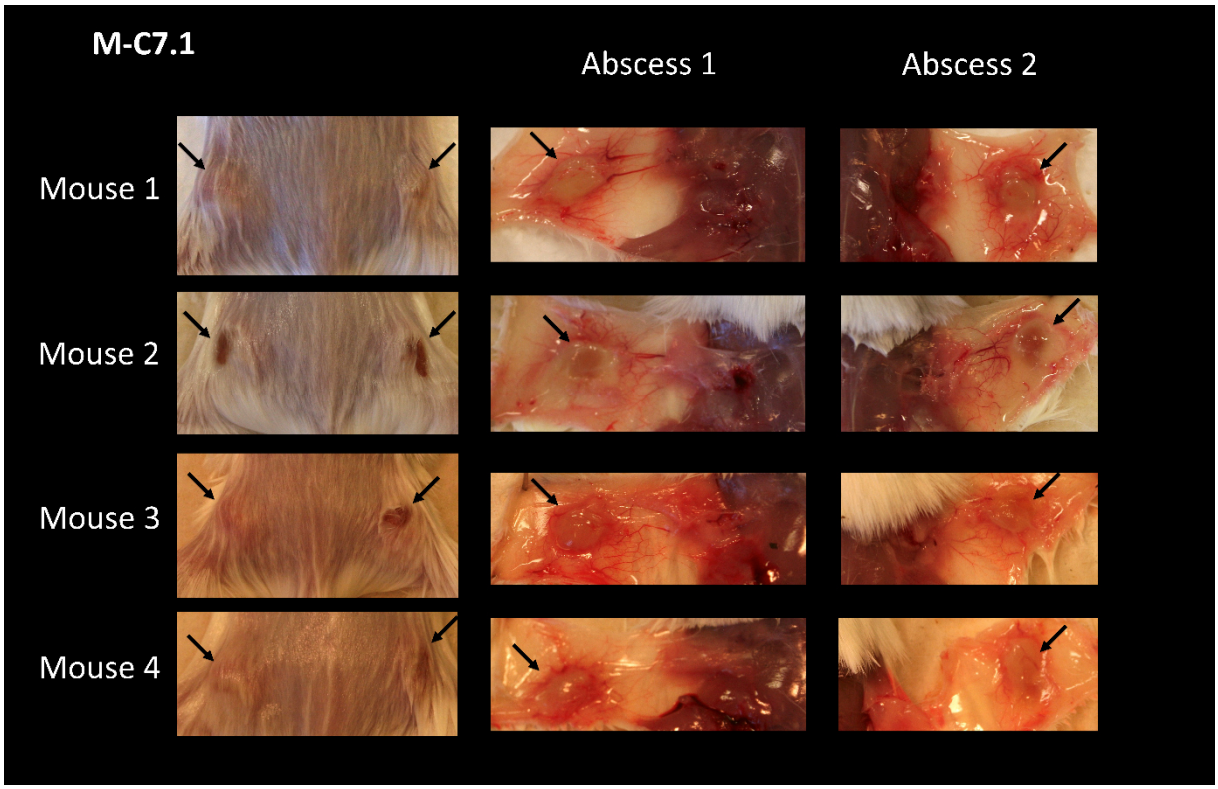

Supplemental Figure S4B. Visual phenotypes of all mouse skin abscesses caused by USA300 WT treated with M-C7.1. Abscesses indicated by black arrows, abscess 1 represents the opened right abscess, abscess 2 represents the opened left abscess.

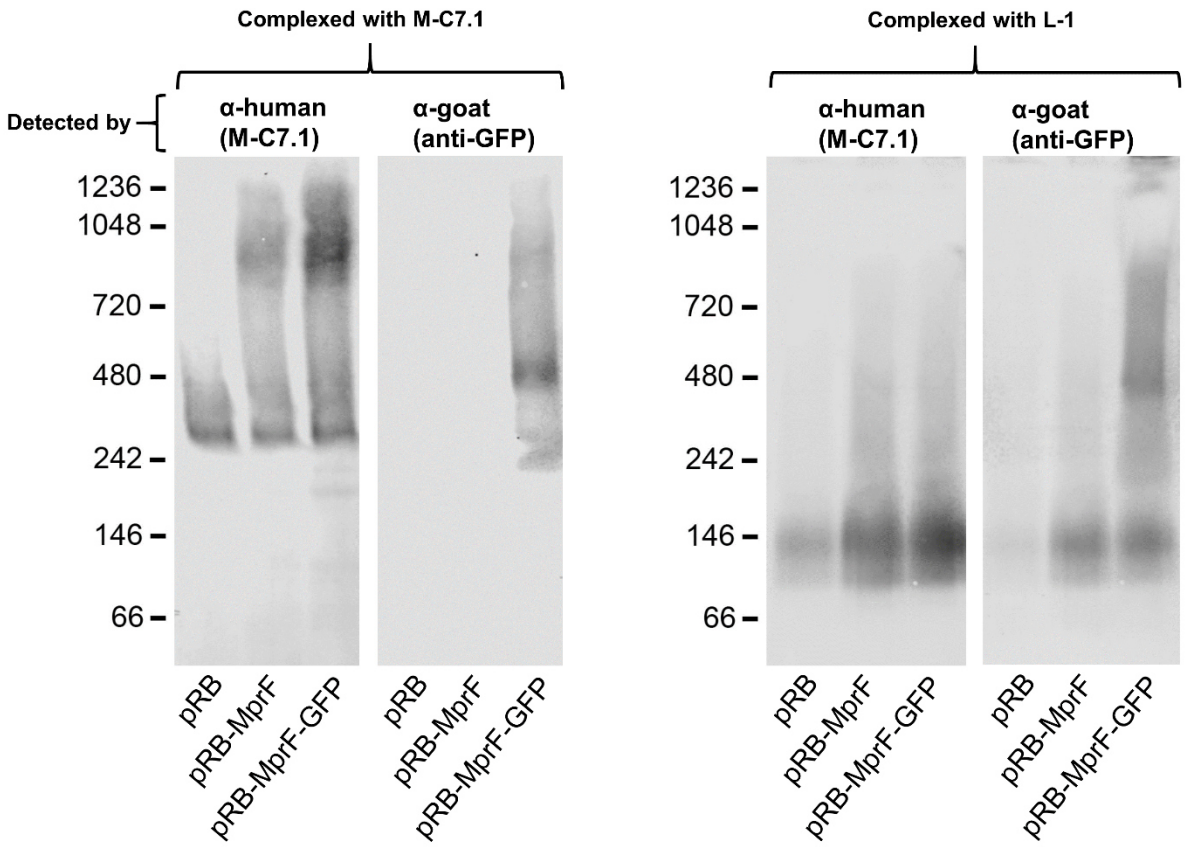

851

852 **Supplemental Figure S5.** Detection of M-C7.1 binding to MprF. Single channels are showed in black

853 and white from figure 3A. Further explanations are found in figure legend of figure 3A.

854

855

856 **Supplemental tables**

857

858 **Table S1**. MprF-directed antibodies and its target peptides.

Antibody	Antigen	Peptide sequence	Framework
M-C1	Cyclic peptide, loop TMS 1-2	ELSGINFKDTLVEFSKINR	VH3-23 kappa 3
M-C7.1	Cyclic peptide, loop TMS 7-8	LGFKTLGVPEEKV	VH1A kappa 1
M-C7.2	Cyclic peptide, loop TMS 7-8	LGFKTLGVPEEKV	VH3-23 kappa 1
M-C7.3	Cyclic peptide, loop TMS 7-8	LGFKTLGVPEEKV	VH1A kappa 1
M-C9.1	Cyclic peptide, loop TMS 9-10	DALYDGNHLT	VH1A kappa 1
M-C9.2	Cyclic peptide, loop TMS 9-10	DALYDGNHLT	VH3-23 kappa 1
M-C13.1	Cyclic peptide, loop TMS 13-14	DIYTIEMHTSVLR	VH1A kappa 1
M-C13.2	Cyclic peptide, loop TMS 13-14	DIYTIEMHTSVLR	VH1A kappa 1

859

860 **Table S2.** Bacterial strains used in this study.

Strain name	Characteristics
S. aureus SA113 WT (ATCC 35556)	Restriction-deficient *S. aureus* strain derived from NCTC 8325 (Iordanescu & Surdeanu, 1976)
S. aureus SA113*ΔmprF*	MprF deletion mutant of SA113, Erm^r (Peschel et al., 2001)
S. aureus SA113*Δspa*	Spa deletion mutant of SA113. Constructed in this study. Markerless.
S. aureus SA113*ΔspaΔmprF*	Spa and MprF double deletion mutant of SA113. Constructed in this study. Erm^r
S. aureus DAP-R MRSA 703	Daptomycin resistant clinical MRSA isolate possessing a single point mutation in *mprF* (S295L) (Jones et al., 2008)
S. aureus USA300 LAC	CA-MRSA wild type strain (Wang et al., 2007)
E. coli TG1	Strain for phage display usage (Prassler et al., 2011)

861

862 **Table S3.** Plasmids used in this study.

Plasmid	Characteristics	Short name in figures
pKOR1	*E. coli/S. aureus* shuttle vector to allow allelic replacement with inducible counter-selection in staphylococci (Bae & Schneewind, 2006)	-
pRB474	*E. coli/S. aureus* shuttle vector pRB474 (Bruckner, 1992)	pRB
pRB474mprF	*mprF* cloned in *E. coli/S. aureus* shuttle vector pRB474 (Peschel et al., 2001)	pRB-MprF
pRB474mprF-GFP	N-terminally GFP tagged *mprF* cloned in *E. coli/S. aureus* shuttle vector pRB474 (Ernst et al., 2015)	pRB-MprF-GFP
pRB474mprFdelCys flag	C-terminally FLAG tagged, cysteine depleted *mprF* cloned in *E. coli/S. aureus* shuttle vector pRB474; constructed in this study	WT (-Cys)
pRB474mprFdelCys T263C flag	C-terminally FLAG tagged, cysteine depleted *mprF* with artificial cysteine insertion cloned in *E. coli/S. aureus* shuttle vector pRB474; as indicated, each plasmid bears another amino acid substituted against cysteine (e.g. T263C)	pRB-T263C
pRB474mprFdelCys A99C flag		pRB-A99C
pRB474mprFdelCys T480C flag		pRB-T480C

863

864

865 **Table S4.** Primers used in this study.

Primer	5' → 3' sequence	Usage
A99C fw	GCATTGAATTGTATTGTAGGTTTCGGTGGCTTTATTGGTGCAGGCG	Forward primer for construction of pRB-A99C by site-directed mutagenesis
A99C rev	CCGAAACCTACAATACAATTCAATGCATTGATGATATAACTTACTC	Reverse primer for construction of pRB-A99C by site-directed mutagenesis
T263C fw	GTTGTATTACTAGGATTTAAATGTTTAGGTGTCCCTGAGGAAAAAG	Forward primer for construction of pRB-T263C by site-directed mutagenesis
T263C rev	CTTTTTCCTCAGGGACACCTAAACATTTAAATCCTAGTAATACAAC	Reverse primer for construction of pRB-T263C by site-directed mutagenesis
T480C fw	GGAACGTTATATGCATTAGATATTTATTGTATTGAAATGCATACATCTGTATTGCG	Forward primer for construction of pRB-T480C by site-directed mutagenesis
T480C rev	CGCAATACAGATGTATGCATTTCAATACAATAAATATCTAATGCATATAACGTTCC	Reverse primer for construction of pRB-T480C by site-directed mutagenesis
mprF C199+204S fw	TACTCTACTTTAGTGTCGTCTGTTGAATGGTTAGCAG	Primer for cysteine depletion of pRB474 encoded native *mprF* by site-directed mutagenesis
mprF C199+204S rev	AACAGACGACACTAAAGTAGAGTACAATCCTACAAAACG	
mprF C217A fw	TTCGCTGGTGTAATTGTTGACGC	
mprF C217A rev	ACCAGCGAAATATAATACAACTGC	
mprF C380A fw	GCTGCTTTATTACTTTTACTGAATGTAGTTGG	
mprF C380A rev	TAAAGCAGCACTAGTATGAATTGCC	
mprF C526S fw	GATAGCGAGGAGATTATTAATCAG	
mprF C526S rev	CTCGCTATCTTCAATTTTAGAAG	
mprF C717S fw	GTAATTGCATTTAGTAGTTTAATGCCAACATACTTTAATGATG	
mprF C717S rev	CTACTAAATGCAATTACTTCATTTTCTTCATTTCGCATTACACC	
Spa-del_attB1	GGGGACAAGTTTGTACAAAAAAGCAGGCCAATATTCCATGGTCCAGAACT	Construction of a markerless *spa* knockout mutant using the pKOR1 vector system (Bae & Schneewind, 2006)
Spa-del	GTCGAGATCTATAAAAACAAACAATACACAACG	
Spa-del_attB2	GGGGACCACTTTGTACAAGAAAGCTGGGATCAGCAAGAAAACACACTTCC	
Spa-del rev	AAAAGATCTAACGAATTATGTATTGCAATA	

866

867

868 **Supplemental references**

869 Bae T, Schneewind O (2006) Allelic replacement in Staphylococcus aureus with inducible counter-
870 selection. *Plasmid* 55: 58-63
871 Bruckner R (1992) A series of shuttle vectors for Bacillus subtilis and Escherichia coli. *Gene* 122: 187-
872 92
873 Ernst CM, Kuhn S, Slavetinsky CJ, Krismer B, Heilbronner S, Gekeler C, Kraus D, Wagner S, Peschel A
874 (2015) The lipid-modifying multiple peptide resistance factor is an oligomer consisting of distinct
875 interacting synthase and flippase subunits. *MBio* 6
876 Iordanescu S, Surdeanu M (1976) Two restriction and modification systems in Staphylococcus aureus
877 NCTC8325. *J Gen Microbiol* 96: 277-81
878 Jones T, Yeaman MR, Sakoulas G, Yang SJ, Proctor RA, Sahl HG, Schrenzel J, Xiong YQ, Bayer AS (2008)
879 Failures in clinical treatment of Staphylococcus aureus Infection with daptomycin are associated with
880 alterations in surface charge, membrane phospholipid asymmetry, and drug binding. *Antimicrob*
881 *Agents Chemother* 52: 269-78
882 Peschel A, Jack RW, Otto M, Collins LV, Staubitz P, Nicholson G, Kalbacher H, Nieuwenhuizen WF,
883 Jung G, Tarkowski A, van Kessel KP, van Strijp JA (2001) Staphylococcus aureus resistance to human
884 defensins and evasion of neutrophil killing via the novel virulence factor MprF is based on
885 modification of membrane lipids with l-lysine. *J Exp Med* 193: 1067-76
886 Prassler J, Thiel S, Pracht C, Polzer A, Peters S, Bauer M, Norenberg S, Stark Y, Kolln J, Popp A,
887 Urlinger S, Enzelberger M (2011) HuCAL PLATINUM, a synthetic Fab library optimized for sequence
888 diversity and superior performance in mammalian expression systems. *J Mol Biol* 413: 261-78
889 Wang R, Braughton KR, Kretschmer D, Bach TH, Queck SY, Li M, Kennedy AD, Dorward DW, Klebanoff
890 SJ, Peschel A, DeLeo FR, Otto M (2007) Identification of novel cytolytic peptides as key virulence
891 determinants for community-associated MRSA. *Nat Med* 13: 1510-4

892